INSTITUTO SUPERIOR DE ENGENHARIA DO PORTO
MESTRADO EM ENGENHARIA BIOMÉDICA



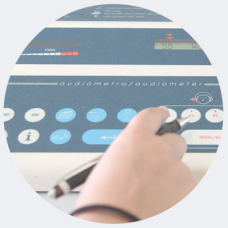


BIOINSPIRED ELECTROCHEMICAL PLATFORM FOR DETECTION OF INFLAMMATION-RELATED BIOMARKERS

BEATRIZ OLIVEIRA MOREIRA
outubro de 2023

Instituto Superior de Engenharia do Porto

BIOINSPIRED ELECTROCHEMICAL PLATFORM FOR DETECTION OF INFLAMMATION-RELATED BIOMARKERS

Beatriz Oliveira Moreira

2023

Porto School of Engineering

Physics Department

P.PORTO


P.PORTO

Instituto Superior de Engenharia do Porto

BIOINSPIRED ELECTROCHEMICAL PLATFORM FOR DETECTION OF INFLAMMATION-RELATED BIOMARKERS

Beatriz Oliveira Moreira

Student n.º 1210158

Thesis presented to the Porto School of Engineering for the degree of Master's in Biomedical Engineering, under the supervision of Doctor Gabriela Vasconcelos Martins and co-supervision of Doctor Maria Arcelina Marques.

2023

Porto School of Engineering

Physics Department

P.PORTO


P.PORTO

ACKNOWLEDGMENTS

It is with a great sense of satisfaction and fulfilment that I deliver this work. The completion of this dissertation marks the end of an important stage in my life and as such, I would like to thank all those who have accompanied me.

First, I would like to start by expressing my gratitude to the Polytechnic of Porto - School of Engineering (ISEP). The opportunity to do my master's degree at this institution was a privilege, and I am grateful for the knowledge and skills I acquired during my time here.

Next, I would like to extend my thanks to my supervisors, Dra Arcelina Marques, and Dra Gabriela Martins. Your guidance and expertise were invaluable throughout the process of completing my master's thesis. Thank you for all your support and words of friendship during this period.

I would also like to express my gratitude to the BioMark Research Group for providing me with a stimulating environment and the opportunity to apply my skills and knowledge to challenging projects. The experience I have gained during my time here has been invaluable to my professional growth. To Dra Felismina Moreira, for welcoming me to Biomark and for always monitoring my work and ensuring that I had the best experience.

I also want to thank my friends, Raquel Pereira, Raquel Vaz, Catarina Santos, Daniela Oliveira, and Marta Dias, who have made BioMark seem like a second home and who I will always have by my side.

To Inês Vinagre for being my best buddy for the past two years and for always encouraging me.

To my sister for always giving me a word of support at the right time, for always being there for me, for being the best big sister anyone could ask for and for never letting me fall.

To my parents, for always encouraging me in all my choices, for never letting me give up when I didn't think I could make it and for always being there for me.

To my boyfriend, Ivo, for all your patience with me, for never giving up on me and always seeing the best in me. Thank you!

The lessons and experiences I've learnt over the years will be with me all my life.

ABSTRACT

An adaptive reaction known as inflammation is typically brought on by unpleasant stimuli and diseases such as widespread infection and/or tissue damage. The immune system launches an inflammatory reaction as a defensive strategy, producing cells and cytokines to combat these invaders, which may cause discomfort, redness, swelling, and bruising. In particular, the liver produces the biomolecule C-Reactive Protein (CRP) in reaction to cytokines that are generated during inflammatory and infectious processes. In this situation, the creation of straightforward, affordable, and user-friendly diagnostic instruments to check for inflammatory biomarkers at the point of treatment might be very beneficial for therapeutic purposes.

The goal of this research is to create an electrochemical biosensor with exceptional sensitivity that can monitor CRP. The molecularly imprinted polymer (MIP), which serves as the biorecognition component of the biosensor, is formed by electrochemically polymerizing a combination of aniline and chitosan in the presence of the target protein, CRP. Here, adding chitosan to the monomer mixture significantly improves the biosensor's stability and repeatability. The bulk technique, which offers a straightforward, quick, one-step procedure for altering and assessing various variables, was used to assemble the polymeric film by means of electropolymerization. It is feasible to model and control the thickness and porosity of the produced polymeric film by changing and adjusting electropolymerization process parameters including the scanning rate and the number of cycles. The scanning speed chosen for the studies was 0.5 Vs^{-1} and the number of electropolymerization cycles optimised was 5 cycles.

After electrochemical synthesis, CRP was successfully removed from the polymeric network using acid-organic combinations, allowing cavities that are complementary in size and shape to the target molecule to develop. Electrochemical impedance spectroscopy (EIS) was used to assess the electrochemical performance while the biosensor assembly was being optimized.

The imprinting effect was subsequently demonstrated by examining the electrochemical detection properties, and the improved biosensor showed a linear electrochemical response in the concentration range of 0.001 ng mL^{-1} to 0.01 μg mL^{-1} and a LOD of 2.22 pg mL^{-1}. Furthermore, surface alterations on the gold electrode were validated by chemical and morphological characterizations like Scanning Electron Microscopy (SEM), Fourier Transform Infrared Spectroscopy (FTIR) and Raman techniques. In terms of sensitivity, stability, and repeatability, the final biosensor device showed significant promise, making it a more convenient and affordable alternative for monitoring chronic wounds progression.

KEYWORDS

Biosensor; Molecularly imprinted polymer; Gold-based electrodes; Electrochemical detection; C-Reactive Protein.

RESUMO

A inflamação é normalmente provocada por estímulos desagradáveis e doenças como a infeção generalizada e/ou danos nos tecidos. O sistema imunitário desencadeia uma reação inflamatória como estratégia de defesa, produzindo células e citocinas para combater estes invasores, o que pode causar desconforto, vermelhidão, inchaço e hematomas. Em particular, o fígado produz a biomolécula Proteína C-Reativa (CRP) em reação às citocinas que são geradas durante os processos inflamatórios e infeciosos. Nesta situação, o desenvolvimento de instrumentos de diagnóstico simples, económicos e fáceis de utilizar para verificar a presença de biomarcadores inflamatórios no local do tratamento pode ser muito benéfico do ponto de vista terapêutico.

O objetivo deste trabalho é desenvolver um biossensor eletroquímico com uma boa sensibilidade que possa monitorizar a CRP. O polímero de impressão molecular (MIP), que serve como componente de biorreconhecimento do biossensor, é formado pela polimerização eletroquímica de uma combinação de anilina e quitosano na presença da proteína alvo, a CRP. Neste caso, a introdução de quitosano na mistura de monómeros melhora significativamente a estabilidade e a reprodutibilidade do biossensor.

A técnica *bulk*, oferece um procedimento simples, rápido num só passo para alterar e avaliar diversas variáveis, permitindo o fabrico do material polimérico através da utilização da técnica de electropolimerização. É possível modelar e controlar a espessura e a porosidade da película polimérica produzida, alterando e ajustando os parâmetros do processo de electropolimerização, incluindo a velocidade de varrimento e o número de ciclos. A velocidade de varrimento escolhida para a realização dos estudos foi de 0.5 Vs^{-1} e o número de ciclos de electropolimerização otimizado foi de 5 ciclos.

Após a síntese eletroquímica, a CRP foi removida com sucesso da rede polimérica utilizando combinações ácido-orgânicas, permitindo o desenvolvimento de cavidades complementares em tamanho e forma à molécula alvo. A espetroscopia de impedância eletroquímica (EIS) foi utilizada para avaliar o desempenho eletroquímico enquanto a construção do biossensor estava a ser otimizado.

O resultado da impressão molecular foi subsequentemente demonstrado através da avaliação das propriedades de deteção eletroquímica e o biossensor otimizado apresentou uma resposta eletroquímica linear no intervalo de concentração de 0.001 ng mL^{-1} a 0.01 μg mL^{-1} e um LOD de 2.22 pg mL^{-1}. Além disso, as alterações estruturais na superfície do eléctrodo de ouro foram validadas por caracterizações químicas e morfológicas como Microscopia eletrónica de varrimento (SEM), espetroscopia de infravermelhos com transformada de Fourier (FTIR) e técnicas Raman. Em termos de sensibilidade, estabilidade e repetibilidade, o dispositivo biossensor final mostrou-se significativamente promissor, tornando-o uma conveniente e acessível ferramenta para a monitorização remota da progressão de feridas crónicas.

PALAVRAS-CHAVE

Biossensor; Polímero de impressão molecular; Elétrodos de ouro; Deteção eletroquímica; Proteína C-Reativa.

CONTENTS

LIST OF FIGURES

LIST OF TABLES

LISTS OF ACRONYMS AND SYMBOLS

Lists of Acronyms

ATR	Attenuated Total Reflectance
CE	Counter electrode
COF	Covalent Organic Frameworks
CRP	C-Reative Protein
CV	Cyclic voltammetry
DNA	Deoxyribonucleic Acid
EIS	Electrochemical impedance spectroscopy
ESR	Erythrocyte Sedimention Rate
FTIR	Fourier transform infrared spectroscopy
GE	Germanium
HPLC	High Performance Liquid Chromatography
IgA	Immunoglobulin A
IgD	Immunoglobulin D
IgE	Immunoglobulin E
IgG	Immunoglobulin G
IgM	Immunoglobulin M
IF	Imprinting Factor
IL-1	Interleukin-1
IL-12	Interleukin-12
IL-6	Interleukin-6
ISEP	School of Engineering of Polytechnique School of Porto
LOD	Limit of Detection
MIP	Molecularly imprinted polymer
MOF	Metal-Organic Frameworks
NIP	Non-imprinted polymers
pI	Isoelectric Point
POC	Point-of-care
PV	Plasma Viscosity
RE	Reference electrode
SEM	Scanning electron microscope
SPE	Screen-printed electrode
SWV	Square wave voltammetry
TNF	Tumor Necrosis Factor
WE	Working electrode

Lists of Symbols

Rct	Charge-transfer resistance	KΩ
R	Resistance	Ω
V	Voltage	$Volts$
σ	Standard deviation	

1. INTRODUCTION

This chapter provides a brief introduction to the problem being addressed in this thesis. It highlights the main objectives of the study, discusses the selection of the used methodology, and supplies some information regarding the research center where the investigation was developed. In addition, an outline of the work is also included.

1.1. Problem Statement

Typically, inflammation is a responsive mechanism that the body employs when exposed to harmful stimuli or conditions, such as tissue damage or/ and infection [1]. When the body is confronted with external threats like bacteria, viruses, or toxins, inflammation can arise. As a consequence, the immune system releases cytokines and inflammatory cells to combat these invaders. Pain, swelling, bruising, or redness may be some of the outcomes of inflammation event [2]. Discomfort is usually temporary and disappears when the inflammatory response has done its job. But in some instances, inflammation can persist and cause harm [3], evolving to a severe chronic state.

During inflammation, white blood cells accumulate at the site of injury, primarily phagocytes that ingest bacteria and foreign particles to clean up cellular debris. Neutrophils, a type of phagocyte, are involved in acute inflammation and contain cell-destroying enzymes and proteins. If tissue damage is minor, an adequate supply of neutrophils is obtained from circulating blood. However, in severe damage, immature neutrophils are released from the bone marrow [3]. Under this context, two types of inflammation can occur: acute (short lived) inflammation and chronic (long-lasting) inflammation [4].

Acute inflammation begins after a specific injury that will cause soluble mediators such as cytokines, acute phase proteins, and chemokines to promote the migration of neutrophils and macrophages to the area of inflammation. These cells are part of a natural innate immunity that can play an active role in acute inflammation [4].

In chronic infection the body continues to send out inflammatory cells, even when there is no longer any danger. The stimulus may be low virulence infectious agents or alterations in host tissue due to responses to endogenous components (e.g., metabolites and autoimmune alterations). In contrast to acute inflammatory where responses are characterized primarily by the recruitment of neutrophils from the blood, chronic inflammation is characterized by the continued recruitment of circulating mononuclear leukocytes, including monocytes and populations of T lymphocytes [5]. Common symptoms of chronic inflammation include fatigue; body pain; depression or anxiety; gastrointestinal complications (diarrhea or constipation); weight gain; weight loss; persistent infections. These symptoms can range from mild to severe and last for several months or years [6], [7], which constitute a significant impact in health and quality of life of patients.

Currently, the development of innovative, quick, and easy-to-use methodologies for inflammation monitoring are still needed. In this context, C-reactive protein (CRP) is an acute inflammatory protein that increases up to 1,000-fold at sites of infection or inflammation. CRP is produced as a homopentameric protein, termed native CRP, which can irreversibly dissociate at sites of inflammation and infection into five separate monomers, termed monomeric CRP [8]. CRP is synthesized primarily in liver hepatocytes but also by smooth muscle cells, macrophages, endothelial cells, lymphocytes, and adipocytes [8]. Thus, tracking in-situ the levels of CRP biomarker can be highly valuable from a therapeutic point-of-view.

The detection of inflammation events remains a challenge for healthcare providers as there are limited quick, practical, and cost-effective methods available. This creates a burden on laboratories and healthcare systems, leading to delayed diagnosis and treatment of patients. To address this challenge, there is an urgent need to explore innovative solutions that can enable rapid and accurate monitorization of inflammation, particularly in point-of-care (POC) settings. These solutions should not only be affordable but also easy to implement, enabling healthcare providers to diagnose locally quickly and efficiently inflammation in patients.

In the last decades, biosensors have experienced important applications in medical diagnostics, personalized medicine, food industry, and substance testing laboratories [9]. One of the main advantages of using biosensing technology is the ability to detect low concentrations of a target analyte in a complex biological sample. Moreover, biosensor devices are becoming increasingly advanced, sophisticated, inexpensive, and miniaturized [9]. However, there is still an acute need for simple and sensitive biosensing approaches that can be employed in a POC context. Particularly, this work aims to develop and study an innovative electrochemical biosensing platform to detect and quantify CRP presence in POC, with particular emphasis in wound applications.

1.2. Objectives and Research questions

The main objective of this thesis is to develop a sensitive and selective electrochemical biosensor using molecularly imprinted polymers (MIPs) as the biorecognition element for the detection of CRP protein.

This work was developed keeping in mind the research question, "How best to develop a selective, stable and reproducible biosensor?"

To pursue the general objective of this research, the following specific objectives were formulated:

- To achieve a linear response higher than 98%;
- To reach an electrochemical response with high reproducibility and selectivity;
- To fabricate a biosensor holding elevated stability and robustness.

1.3. Methodological options

For the development of this thesis some methodological decisions were made such as:

- The use of chitosan biopolymer in the implementation of the monomer mixture since it is expected to provide great stability and reproducibility to the biosensor assembly.
- The use of electrochemical polymerization due to its simplicity, robustness, and possibility of working over a wide range of solvents, temperature and mild conditions.
- The use of cyclic voltammetry (CV) and electrochemical impedance spectroscopy (EIS) as electrochemical techniques, since these are widely used and recognized for their good sensitivity performance.

1.4. Biomark presentation

This thesis was developed by framing the research group BioMark Sensor Research. This research group, integrated in the School of Engineering - Polytechnic of Porto (ISEP), aims the development, modification, and characterization of novel (bio)materials with their own functionalities and application in the Medical and Industrial context, in transversal domains such as Bioengineering, Materials Science,

Electrical Engineering, Mechanical Engineering and Chemical Engineering [10]. Furthermore, BioMark research team gathers solid experience in the design and optimization of innovative (electrochemical and optical) biosensors for biomarker detection with biological relevance, mostly targeted for therapeutics/diagnosis applications.

1.5. Outline

This work presents 4 chapters in addition to the Introduction.

Chapter 2 focuses exclusively on addressing the theoretical part of the dissertation topic, with a special emphasis on Inflammation and Biosensors, with a description of their components and the various (bio)recognition elements and transducers available. This chapter also presents the state of the art of the existing studies regarding the subject.

Chapter 3 presents the work developed as well as the methodology employed.

Chapter 4 concentrates on the presentation and discussion of the results obtained.

Finally, chapter 5 presents a summary of the developed work as well as future perspectives.

2. LITERATURE REVIEW

This chapter will review the literature to frame the developed work, addressing the topic of Inflammation and Biosensors, and present the state of the art regarding the existing biosensor technology.

2.1. Inflammation

Inflammation is generally defined as a response to stimulation by invading pathogens or endogenous signals such as damaged cells that results in tissue repair or sometimes pathology when the response goes unchecked. However, understanding the mechanisms, context, and role of inflammation during physiological immune responses and pathology is a complex phenomenon, constantly evolving [11]. Inflammation is therefore a defense mechanism that is vital to health maintenance. Usually, during acute inflammatory responses, cellular and molecular events and interactions efficiently minimize, impending injury or infection. This mitigation process contributes to restoration of tissue homeostasis and resolution of the acute inflammation. However, uncontrolled acute inflammation may become chronic, contributing to a variety of chronic inflammatory diseases [12]. The inflammatory response is the coordinate activation of signaling pathways that regulate inflammatory mediator levels in resident tissue cells and inflammatory cells recruited from the blood. Inflammation is a common pathogenesis of many chronic diseases, including cardiovascular and bowel diseases, diabetes, arthritis, and cancer [12]. To prevent progression from acute inflammation to persistent, chronic inflammation, the inflammatory response must be suppressed to prevent additional tissue damage [12].

Recent studies state that chronic inflammation is related to several chronic diseases such as type 2 diabetes mellitus [13], cancer [14], and cardiovascular diseases [15]. Inflammation was also linked to other diseases, such as asthma, cardiac arrhythmia, and depression [16]. Particularly, metabolic diseases are driven by chronic low-grade inflammation characterized by elevated serum levels of proinflammatory cytokines such as Interleukin-1(IL-1), Interleukin-6 (IL-6), Interleukin-12 (IL-12), and Tumor Necrosis Factor (TNF-a); chemokines, including CXCL8, CCL2, CCL3, and CCL5; acute phase reactants such as C-reactive proteins (CRP), serum amyloid A, and ferritin; insulin resistance-associated adipokines such as retinol-binding protein 4 and resistin; and procoagulant factors, including plasminogen activator inhibitor [5]. Furthermore, several risk factors promote a low-level inflammatory response, such as age, obesity, diet, smoking, low sex hormones, stress, and sleep disorders [17].

2.1.1. Types of Chronic Inflammation

Special emphasis will be given herein to chronic inflammation due to the severe consequences in terms of health cost and quality of life that are associated to this type of pathology [6].
There are two types of chronic inflammation:

- **Nonspecific proliferative -** It is characterized by the presence of non-specific granulation tissue formed by infiltration of mononuclear cells (lymphocytes, macrophages, plasma cells) and proliferation of fibroblasts, connective tissue, vessels, and epithelial cells [6].
- **Granulomatous inflammation -** This is a specific type of chronic inflammation characterized by the presence of distinct nodular lesions or granulomas formed with an aggregation of activated macrophages or their derived cell called epithelioid cells usually surrounded by lymphocytes. The macrophages or epithelioid cells within the granulomas often coalesce to form Langhans or giant cells such as foreign body, Aschoff, Reed-Sternberg, and Tumor giant cells. There are two types:

- Granuloma formed due to foreign body or T-cell mediated immune response is termed as foreign body granuloma, for example silicosis [6].
- Granuloma formed due to chronic infection is called infectious granuloma, for example tuberculosis [6].

2.1.2. Inflammatory markers

Inflammatory markers are commonly assessed through blood tests used by healthcare personnel to detect inflammation in the body, caused by many diseases. This can include infections, auto-immune conditions, and cancers. Nowadays, the three most used inflammatory markers are CRP, erythrocyte sedimentation rate (ESR) and plasma viscosity (PV) [18].

- **Blood test for CRP -** When the body responds to infection or inflammation, it generates specific proteins. One such protein is CRP, which is produced by the liver and tends to increase during inflammation. Normally, a CRP value of less than 3 mg L^{-1} is considered normal. However, a value above this may indicate an increased risk of cardiovascular disease, though inflammation in the body can also cause CRP levels to rise to 100 mg L^{-1} or higher. A CRP assay is often used to detect or monitor inflammation in acute or chronic conditions, such as, infections caused by bacteria or viruses, inflammatory bowel disease, autoimmune disorders like lupus, rheumatoid arthritis, and vasculitis, as well as lung diseases like asthma [19].
- **Red cell sedimentation rate (sed rate or ESR) -** This test measures how quickly red blood cells settle to the bottom of a vertical tube of blood. When there is inflammation, red blood cells fall faster, because greater amounts of protein in the blood cause these cells to clump together. Although ranges vary by laboratory, a normal result is usually 20 mm hr^{-1} or less for men and 0-29 mm hr^{-1} for women, while a value over 100 mm hr^{-1} is quite high [20].
- **Plasma Viscosity –** This test measures the viscosity, or the 'thicknesses of the plasma (the liquid part of the blood). Plasma viscosity is affected by the number of proteins in the blood. Protein levels in the blood can increase as part of the normal response to infection or inflammation. Plasma viscosity also increases in certain diseases where proteins (called 'paraproteins') are produced abnormally. Measuring the viscosity of blood may be used to detect and monitor inflammation [21]. The normal range for adults is 1.50-1.72 mPA [22].

2.1.2.1. C- Reactive Protein (CRP)

CRP was identified from patients with acute pneumococcal pneumonia, a name that reflects its reaction with the C-polysaccharide of Pneumococcus. This native protein has five non-covalently bonded and non-glycosylated identical subunits of 206 amino acids each (monomeric) to form a disk-shaped pentagon, or pentameric form [23] (Figure 1).

CRP is a biomarker of inflammation that is extensively used in clinical practice. This protein is an acute-phase protein synthesized by hepatocytes in response to pro-inflammatory cytokines during inflammatory/infectious processes. CRP exists in conformationally distinct forms such as the native pentameric CRP and monomeric CRP and may bind to distinct receptors and lipid rafts and exhibit different functional properties [24].

Higher CRP concentrations may be indicative of an acute infection or inflammation. Higher CRP concentration over time, rather than spikes in CRP, may result in cardiovascular diseases and problems leading to atherosclerosis. Furthermore, some chronic inflammatory diseases like hemorrhagic stroke, Alzheimer's disease, and Parkinson's disease are also associated with CRP formation [24].

Some basic research shows that the inflammatory response plays a central role in various phases of atherosclerosis. From the initial recruitment of circulating leukocytes to the arterial wall to the rupture

of unstable plaques, thereby resulting in the clinical manifestations of the disease. CRP may be critically involved in each of these stages by directly influencing processes, including complement activation, apoptosis, endothelial nitric oxide synthase inhibition, vascular cell activation, monocyte recruitment, lipid accumulation and thrombosis, and pro-inflammatory cytokine formation [24], [25].
CRP plays a vital role in the monitoring of bacterial infection, inflammation, neurodegeneration, tissue injury, and recovery. CRP levels are observed to be increased during acute-phase inflammation as well as chronic inflammatory diseases [24]. The concentration of CRP is measured in milligrams per liter (mg L^{-1}). If the level of CRP is less than 10 mg L^{-1} it is considered normal whereas if it is equal to or greater than 10 mg L^{-1} the person is, then considered to be at higher risk [26].

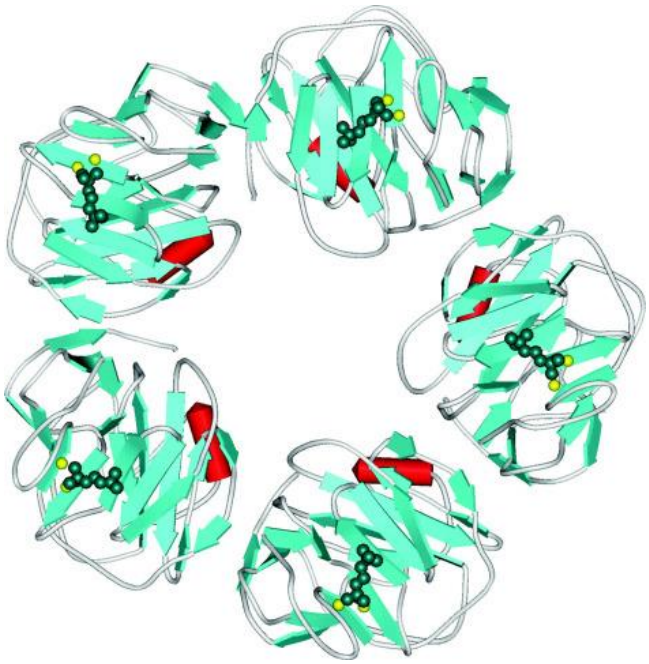

Figure 1- Molecular structure of CRP [27].

2.2. Biosensor

Medicine, biology, and biotechnology all rely heavily on biological and biochemical processes.
According to IUPAC definition, "A biosensor is a self-contained integrated device which can provide specific quantitative or semi-quantitative analytical information using a biological recognition element (biochemical receptor) which is in direct spatial contact with a transducer element. A biosensor should be clearly distinguished from a bioanalytical system, which requires additional processing steps, such as, reagent addition. Furthermore, a biosensor should be distinguished from a bioprobe which is either disposable after one measurement, i.e., single use, or unable to continuously monitor the analyte concentration" [28], [29].
Biosensors are analytical devices for the investigation of bio-material samples to achieve an understanding of their bio-composition, layout, and principle by transforming a biological response into a measurable signal. Figure 2 shows the major areas of applications concerning biosensors.

Figure 2 - Major areas of applications for biosensors [30].

2.2.1. Biosensor Structure

A biosensor consists of an analyte, bioreceptor, transducer, electronics, and display [30], [31]. Figure 3 shows a diagram of the components of a biosensor that includes:

- **Analyte:** An analyte is a substance whose concentration needs to be determined.
- **Bioreceptor:** A molecule that specifically recognizes the analyte is known as a bioreceptor. Enzymes, cells, aptamers, deoxyribonucleic acid (DNA), MIPs and antibodies are some examples of bioreceptors.
- **Transducer:** The transducer is the element that converts one form of energy into another. In a biosensor the role of the transducer is to convert the bio-recognition event into a measurable signal. This process of energy conversion is known as signalization. Most transducers produce either optical or electrical signals that are usually proportional to the amount of analyte–bioreceptor interactions.
- **Electronics:** The main work of this part of a biosensor is to process the transduced signal and make it ready for display. It consists of intricate electronic circuitry that performs signal conditioning such as amplification and translation of signals into the digital form. The processed signals are then evaluated by the display unit of the biosensor.
- **Display (Detector):** The display consists of a user interpretation system such as the liquid crystal display of a computer or a direct printer that generates numbers or curves understandable by the user. This part often consists of a combination of hardware and software that generates results of the biosensor in a user-friendly way. The output signal on the display can be numeric, graphic, tabular or an image, depending on the requirements of the end user.

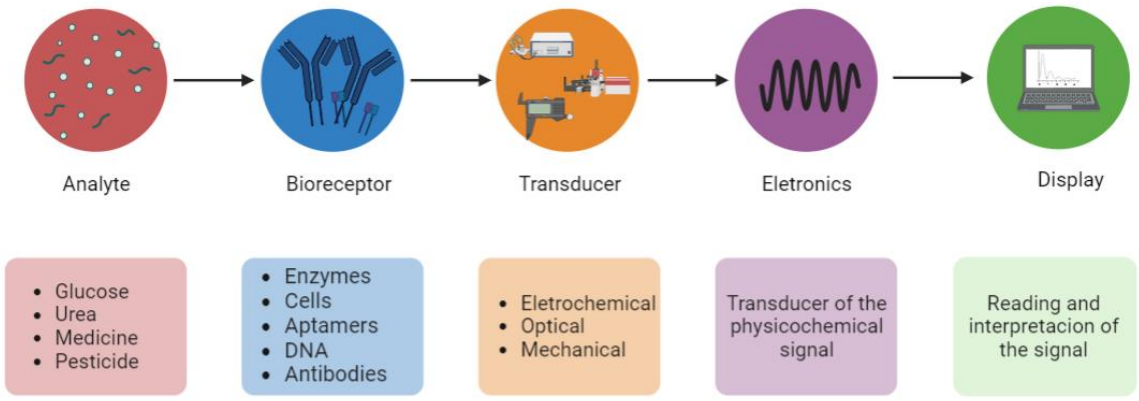

Figure 3 - Diagram of the components of a biosensor.

Biosensors can be categorized according to the basic principles of their transduction signal and biorecognition elements [28].
A few advantages of biosensors are listed below:

- They can measure nonpolar molecules that do not respond to most measurement devices.
- Biosensors are specific due to the immobilized system used in them.
- Rapid and continuous control is possible with biosensors.
- Response time is short (typically less than a minute).
- Practical and easy to use.

Every biosensor possesses a certain set of static and dynamic properties. The performance of the biosensor is affected by the optimization of these features.
Perhaps one of the most crucial components of a biosensor is selectivity. A bioreceptor's selectivity refers to its capacity to identify a particular analyte in a sample that contains various admixtures and pollutants. For instance, the interaction of an antigen and an antibody is the best illustration of selectivity. [30].
The biosensor's reproducibility refers to its capacity to produce the same results under identical testing conditions. When a sample is tested more than once, accuracy refers to the sensor's capability to offer a mean value that is close to the true value while precision refers to the sensor's ability to produce identical findings every time [30].
The stability of a biosensing platform refers to how susceptible it is to environmental disturbances inside and outside of it. A biosensor under measurement may experience a drift in its output signals because of these disruptions. This could skew the concentration being measured and compromise the biosensor's precision and accuracy. In applications where a biosensor needs lengthy incubation periods or ongoing monitoring, stability is the most important component. The reaction of electronics and transducers may be temperature-sensitive, which could affect a biosensor's stability. To achieve a steady response from the sensor, proper tuning of the electronics is necessary. The degree to which the analyte attaches to the bioreceptor—the affinity of the bioreceptor—can also have an impact on stability. High affinity bioreceptors promote the analyte's covalent or strong electrostatic connection, which strengthens a biosensor's stability. The degradation of the bioreceptor over time is another element that has an impact on a measurement's stability [30]. One perfect example of this criteria concerns enzymatic biosensors where the stability and activity of the enzyme element along the time is a crucial factor that affects biosensor performance.

The limit of detection (LOD) or sensitivity of a biosensor is the lowest concentration of analyte that it can detect. A biosensor is necessary in several medical and environmental monitoring applications to confirm the existence of traces of analytes in a sample at analyte concentrations as low as ng ml^{-1} or even fg ml^{-1} [30].

In a mathematical equation, y=mc, where c is the analyte concentration, y is the output signal, and m is the sensitivity of the biosensor, linearity is the property that demonstrates the accuracy of the measured response to a straight line for a set of measurements with various analyte concentrations. The resolution of the biosensor and the range of analyte concentrations under test can both affect the biosensor's linearity. The smallest change in an analyte's concentration necessary to cause a change in the biosensor's response is known. Depending on the application, a good resolution is required as most biosensor applications require not only analyte detection but also measurement of concentrations of analyte over a wide working range [30].

2.2.1.1. Bioreceptor

The primary purpose of a biorecognition element is to provide analyte specificity to a biosensor. The bio-recognition element (e.g., enzyme, antibody, nucleic acid, hormone, organelle, or whole cell), or bioreceptor, is allowed to interact with a specific analyte (e.g., glucose, urea, drug, pesticide, protein) to get a measurable response [31], [32]. Specificity requires a strong and selective affinity between the biorecognition element and target bioanalyte. Several classes of biorecognition elements exist, giving rise to distinct structures that uniquely influence biosensor performance characteristics. As previously mentioned, some examples of bioreceptors include enzymes, cells, aptamers, DNA, MIPs, and antibodies. The advantages and disadvantages of each type of biorecognition element are described in the Figure 4 [31].

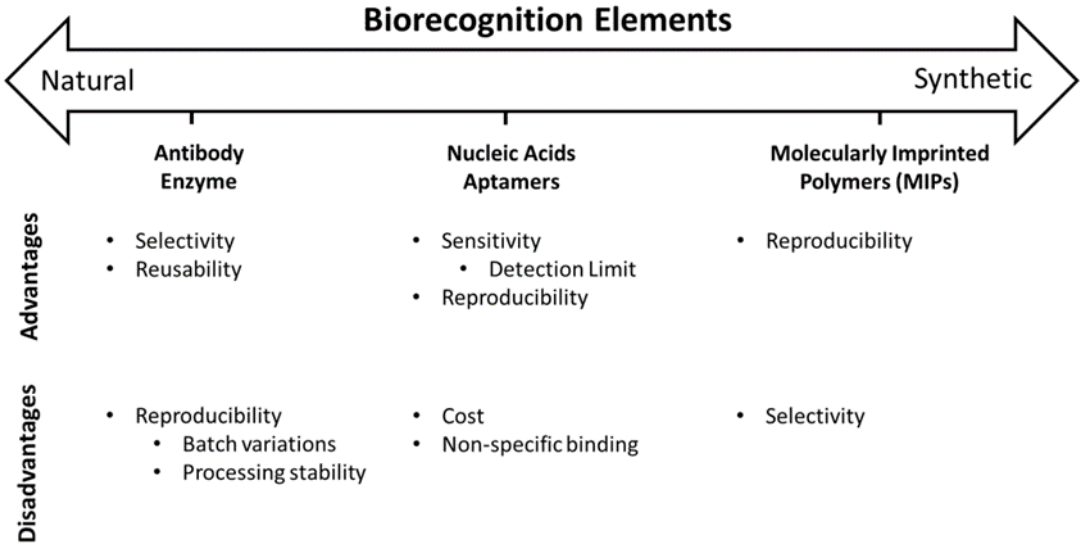

Figure 4- Advantages and disadvantages of each biorecognition element [31].

Antibodies and enzymes are examples of naturally occurring biorecognition components. These biologically derived constructions use physiological interactions that have evolved naturally to produce analyte specificity. Artificially created structures with the ability to replicate physiologically specified interactions are known as synthetic biorecognition elements [31]. Several of these synthetic (bio)molecules have been evaluated from the principles of host-guest chemistry, including the use of

aptamers (aptasensors), MIPs, crown ethers or cyclodextrins; and more recently, the use of metal-organic frameworks (MOFs) or covalent organic frameworks (COFs) has also attracted significant attention as artificial receptors. Among the above list, aptamers and MIPs have clearly demonstrated a high potential and performance, from a commercial point-of-view, but with MIPs still being a cheaper and more versatile option in terms of operation conditions given its higher stability and facile fabrication [33].

2.2.1.1.1. Molecularly Imprinted Polymers (MIPs)

MIPs are best described as synthetic analogues to the natural, biological antibody−antigen systems. As such, they operate by a "lock and key" mechanism to selectively bind the molecule with which they were templated during production [34]. The development of synthetic receptors with comparable specificity and sensitivity to the natural antibody-antigen behavior is a focus of modern sensor research. This molecular recognition holds the possibility of selective, sensitive sensors capable of detecting and monitoring targets in a noninvasive manner, especially when combined with contemporary methods to monitor changes in the recognition elements [34].

Since their beginnings in the 1970s, MIPs have provided the focus for scientists and engineers involved with the development of chromatographic adsorbents, membranes, and sensors [35].

MIPs can be produced for almost any target molecule, which contrasts with the biological systems where the target must match an available antibody, or an antibody must be specifically produced for that target. Moreover, antibodies are more easily produced for macromolecules rather than smaller, molecular targets [34].

The design of MIPs and their use as artificial recognition elements have shown to be successful for targeting both glycans and other molecules. The target molecule, the template, can in fact be a protein, peptide, lipid, amino acid, virus, a cell, nucleic acid, or even more complex glycan structures (Figure 5) [36].

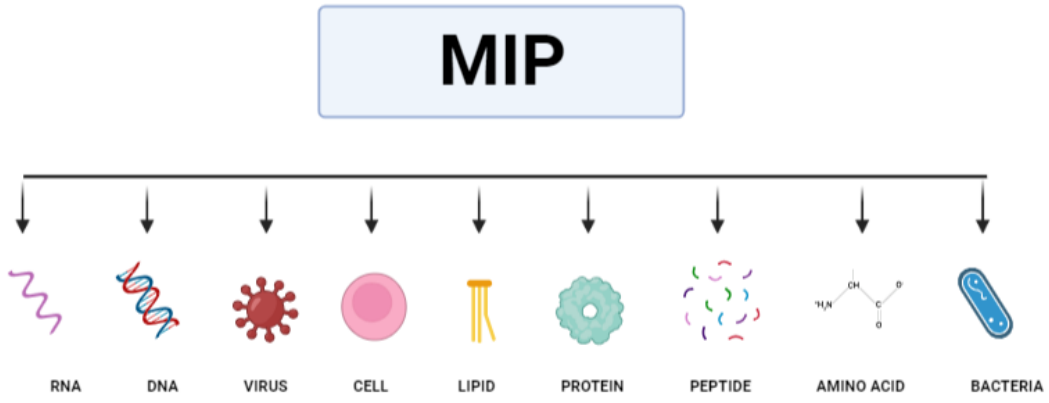

Figure 5- The molecule templates used for imprinting.

Molecular imprinting includes the design and synthesis of the molecular recognition polymers. The imprinting technique is based on (1) the formation and arrangement of the pre-polymerization complex between the template and the functional monomer(s), followed by (2) the synthesis of the polymer matrix on its surroundings, and finally, (3) the template removal. When the template molecule is removed from the imprinted material after polymerization, it leaves behind specific cavities that are complementary to the template in size, shape, and chemical functionality (Figure 6). Some common functional monomers

are acrylamide, methyl methacrylate, methacrylic acid, aniline, pyrrole, among others [34]. MIPs have been used successfully in many applications, including purification [37], isolation [38], chiral separation [39], catalysis [40] and biosensors [41]. Non-imprinted polymers (NIPs) are synthesized in the same manner, but without the presence of the template molecule for comparison purposes [33].

The challenge of designing and synthesizing a MIP is mostly due to the sheer number of experimental variables involved, like the nature and concentration levels of template, functional monomer(s), cross-linker(s), solvent(s) and initiator, the method of initiation and the duration of polymerization [42].

The advantages of working with artificial receptors are not only due to its accessibility, but also to the possibility of working in a wide range of conditions (pH, temperature, solvents, etc.) or outside strict physiological conditions [33]. MIPs represent a promising alternative due to its simple synthesis, comparable performance to affinity bioreceptors, tunability, high stability and low-cost [33]. However, the MIPs have still some limitations, such as time-consuming during optimization stage and complicated preparation process. [35].

MIPs have been used as materials of molecular recognition in many scientific and technical fields, such as solid-phase extraction, chromatograph separation, membrane separations, sensors, drug releases, catalysts, etc [35].

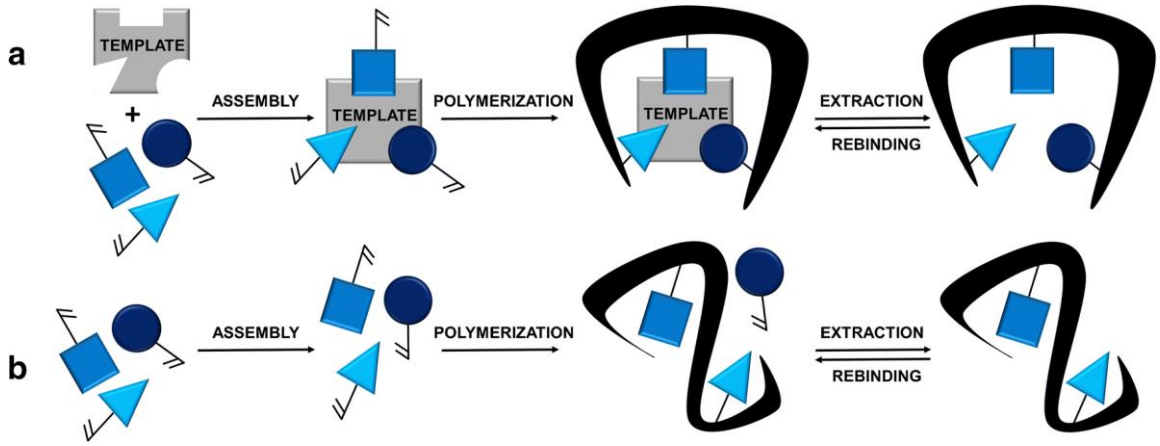

Figure 6- Schematic representation of the synthesis of biomimetic artificial receptors: a) molecularly imprinted polymer (MIP) and b) non-imprinted polymer (NIP) [33].

For the imprinting of molecules on biosensor devices, there are different types of molecular imprinting techniques. The most effective and common methods for developing these materials are bulk imprinting and surface imprinting [43].

In a bulk imprinting strategy, a template molecule is printed on the polymer matrix with a rapid synthetic approach that produces a monolith and, after polymerization, needs to be completely removed from the molecularly imprinted material. This monolith material is usually ground and spliced to obtain polymer fractions with a controllable particle size. In this way, easily accessible model-specific 3D interaction sites within the selective printed polymeric material are obtained [44], [45].

Due to its simplicity, robustness, and the possibility to work over a wide range of solvents, pressure and temperature, this approach is widely used in chromatographic applications, for example for use as column stationary phases in high performance liquid chromatography (HPLC) or in solid phase extraction cartridges [45].

Bulk printing is generally preferred for printing small molecules since, at least in theory, adsorption and release of the template molecule are faster and more reversible, which is an advantage for the reusability of the printed medium for several rounds of analysis [43], [44].

The main drawback stems from the monolithic treatment. On the one hand, these phases are time consuming and there is a loss of polymer during grinding and sieving to a controlled particle size. On the other hand, given the possible damage to its structure during mechanical grinding, there is a risk of altering the print. In addition, the pores are not as accessible as in other approaches, which can also hinder the transport and diffusion of the mass. For this reason, mold removal is more problematic, which is reflected in very poor mold recovery after polymerization [43]–[45].

High affinity recognition sites are formed on the surface of a substrate in surface imprinting. Because of this, recognition sites are more easily accessible with favorable binding kinetics. In other words, template/polymer interactions are not limited to diffusion to the same extent as was a general problem encountered in bulk printing. Therefore, the technique is popular and more applicable especially for the imprinting of biomolecules, including proteins. In surface imprinting, fewer mold molecules are used compared to what is used in conventional imprinting techniques because the mold is only used in the surface coating step in the technique. The main disadvantage of the method in sensor design is the possibility of lower sensitivity compared to bulk imprinting due to the reduced number of imprinted sites. Surface-printed polymers have been widely used for different types of analytes, including proteins, microorganisms, and cells [44].

To summarize, in biosensors, bulk polymerization involves mixing all the required components in a solution, which is then introduced onto the sensor surface to initiate the polymerization process. This technique is simpler and faster. On the other hand, surface polymerization involves adding the components layer by layer onto the sensor surface, making it a more intricate and time-consuming technique.

An important consideration concerns the variety of initiators that can be used to trigger the polymerization reaction, such as, UV light, temperature, or electrical stimulus. Thus, electropolymerization, ultraviolet and thermal polymerization are some of the most common methodologies employed to enable the formation of a polymeric matrix that surrounds a template protein [46], [47].

In particular, electropolymerization has been widely used due to its simplicity, low cost and easy to use technique. Electropolymerization involves the application of a potential or a range of potentials to a solution containing electroactive monomer molecules and/or biomolecules. During this straightforward procedure, the monomer undergoes reduction or oxidation at the electrode surface, generating reactive radical species that subsequently merge to create a polymer [46].

This straightforward method proves to be valuable as it allows for precise control of the polymer thickness by manipulating the electrochemical conditions such as the potential range, number of cycles, and scan rate. Additionally, employing conductive materials of different shapes and sizes further enhances the ability to achieve close control over the polymer thickness [47].

2.2.1.2. Transducer

The transducer is another constituent element of the biosensor, responsible for converting the (bio)recognition event into a measurable signal. The transducer part of the sensor serves to transfer the signal from the output domain of the recognition system, mostly to an optical or electrical domain [48].

Chemical sensors may be classified into three general categories such as optical, piezoelectric, and electrochemical, based on their transduction. Of this, electrochemical transducers become very popular due to ease of measuring and the availability of instrumentation. Moreover, they are found to be effective in offering good LOD, at low cost with the possibility of easy miniaturization and automation [49].

Electrochemical sensors can be classified into several categories including, voltametric, amperometric, potentiometric, impedimetric, photoelectrochemical, and electrogenerated chemiluminescence [50]. Herein, special emphasis will be given to voltametric and impedimetric sensors because these were the electrochemical techniques employed in this Thesis.

Voltametric sensors

- Cyclic Voltammetry (CV)

CV is a routine electrochemical technique used for the determination of electric properties of super capacitors or energy storage devices [51]. This technique is a powerful and popular electrochemical technique commonly employed to investigate the reduction and oxidation processes of molecular species. CV is also valuable to study electron transfer-initiated chemical reactions, which includes catalysis [52]. The x-axis represents a parameter that is imposed on the system, here the applied potential (Voltage), while the y-axis is the response, here the resulting current (Current) passed [52]. The Figure 7 shows a cyclic voltammogram, that is a graphical representation of the current response as a function of the applied potential, where two peaks corresponding to the oxidation and reduction of the chemical species is observed.

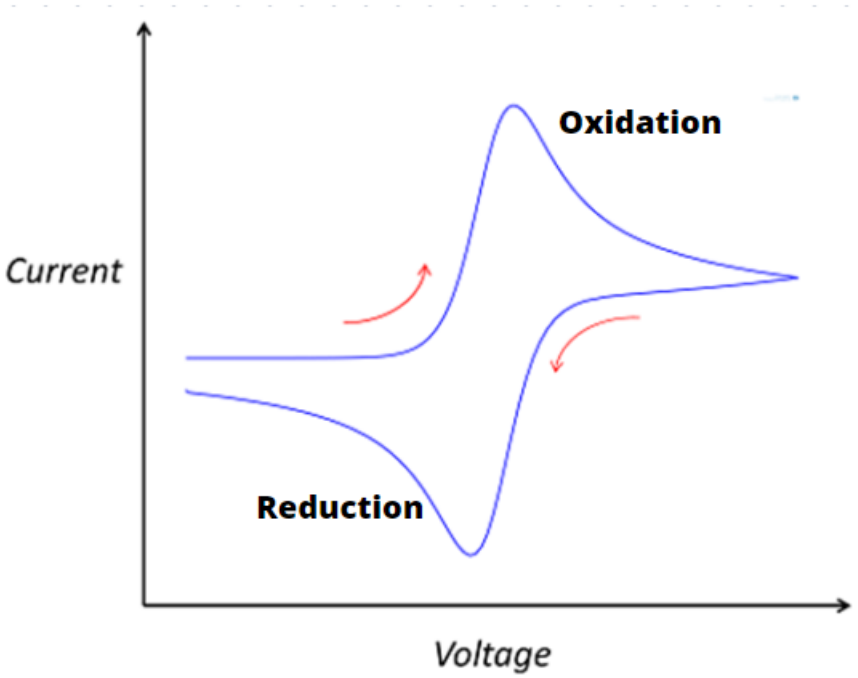

Figure 7 - Cyclic voltammogram acquired by CV [53].

- Square Wave Voltametry (SWV)

Square wave voltammetry (SWV) is one of the fastest and most sensitive techniques, that allows a kinetic and mechanistic evaluation of electrochemical process. In terms of how the technique works, it consists

of defining a potential scale that is modified into square-shaped pulses. Each stage of the potential ramp consists of two opposing potentials, but equal in height. The junction of both potentials gives rise to a SWV cycle, which is repeated several times until generating the typical voltammogram obtained by this technique [52], [54]. The voltammogram obtained results from the relationship between the difference of the two currents and the ramp potential that was applied as can be observed in the Figure 8.

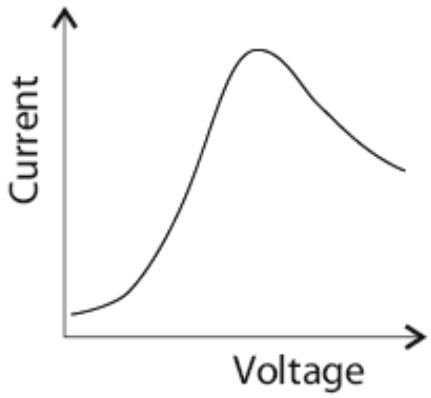

Figure 8 - Representation of square wave voltammogram [55].

Impedimetric Sensors

Electrochemical impedance spectroscopy (EIS) is a powerful technique used for the analysis of interfacial properties related to bio-recognition events occurring at the electrode surface, such as antibody–antigen recognition, substrate–enzyme interaction, or whole cell capturing. EIS offers several advantages reliant on the fact that it is a steady-state technique, that it utilizes small signal analysis, and that it can probe signal relaxations over a very wide range of applied frequency, from less than 1 mHz to greater than 1 MHz, using commercially available electrochemical working stations (potentiostat) [56]. In a conventional electrochemical cell, matter– (redox species)–electrode interactions include the concentration of electroactive species, charge-transfer, and mass-transfer from the bulk solution to the electrode surface in addition to the resistance of the electrolyte. Each of these features is characterized by an electrical circuit that consists of resistances, capacitors, or constant phase elements that are connected in parallel or in a series to form an equivalent circuit. Accordingly, the EIS can study intrinsic material properties or specific processes that could influence conductance, resistance, or capacitance of an electrochemical system. The impedance differs from the resistance, since the resistance observed in DC circuits obeys Ohm's Law directly [56], [57]. The impedance expression is divided into a real part and an imaginary part. When the real part (Z_{real}) is plotted on the X-axis and the imaginary part (Z_{imag}) is plotted on the Y-axis, a "Nyquist Plot" is formed. Each point on the Nyquist plot is an impedance value at a frequency point, while the Z_{imag} is negative. At the X-axis, impedance at the right side of the plot is conducted with low frequency, while, at the higher frequencies, their generated impedances are exerted on the left [56], [58]. Figure 9 shows the schematic of a typical Nyquist plot.

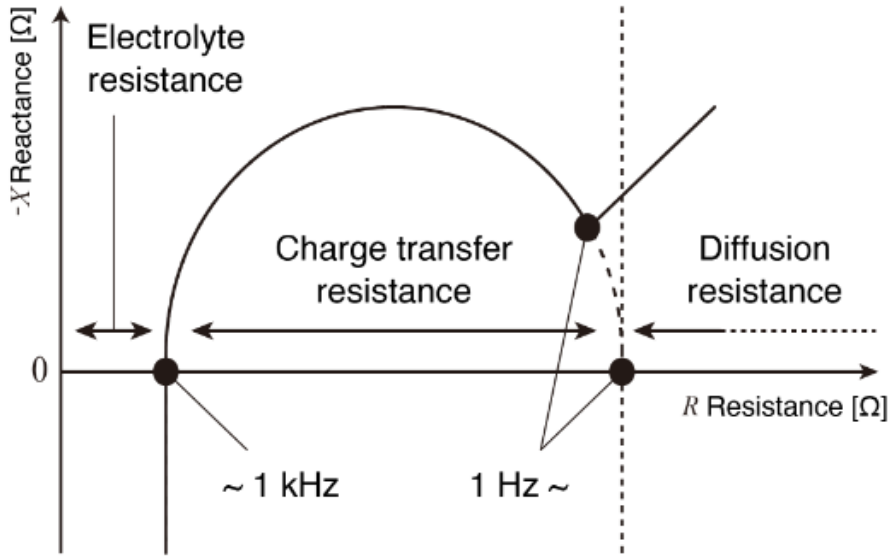

Figure 9 - Typical Nyquist plot [59].

2.2.2. Screen Printed Electrode (SPE)

There is a growing interest in the fabrication of biosensors with high sensitivity, selectivity and efficiency. Biosensors have recently found extensive applications in diverse industries. Currently, many analytical instruments used in environmental, food, pharmaceutical or clinical laboratories and most of the commercial POC devices, can operate using electrochemical sensing technology [60]. In order to perform an electrochemical measurement, it is required an electrochemical cell that combines 2 or 3 electrodes in electrical contact through the same solution interface. In particular, screen-printed technology can be employed to perform layer-by-layer depositions of ink upon a solid substrate, using a screen or mesh. This technology holds great advantages like different geometries and design, flexibility, process automation, good reproducibility and a wide choice of materials available. Screen-printed electrodes (SPEs) present a three-electrode configuration: working (WE), counter (CE) and reference (RE) electrodes printed on the various types of plastic or ceramic substrates, which is easily modifiable with a great variety of commercial or self-made inks [60] (Figure 10).

The WE is the one where the reduction-oxidation reaction takes place and, thus their potential is monitored against the RE potential. Moreover, the RE is kept at a certain distance from the WE so that a stable, known and constant potential is maintained, so that it is possible to determine the potential difference in the system of interest. Finally, the CE is introduced into the electrochemical cell to ensure that the current produced in the system does not interfere with the constant potential of the reference electrode, and by connecting with the electrolytic solution so that the potential can be applied to the WE, thus having to be constituted of a conductive and chemically stable material [61], [62].

There is a wide variety of conductive materials that can be employed as WE, RE and CE, being the most widely used gold (Au), silver (Ag), platinum (Pt) and carbon (C) materials. One of the advantages of electrochemical biosensors is that numerous types of electrodes are available, which can be coupled with a simple, portable electronic system for monitoring [63].

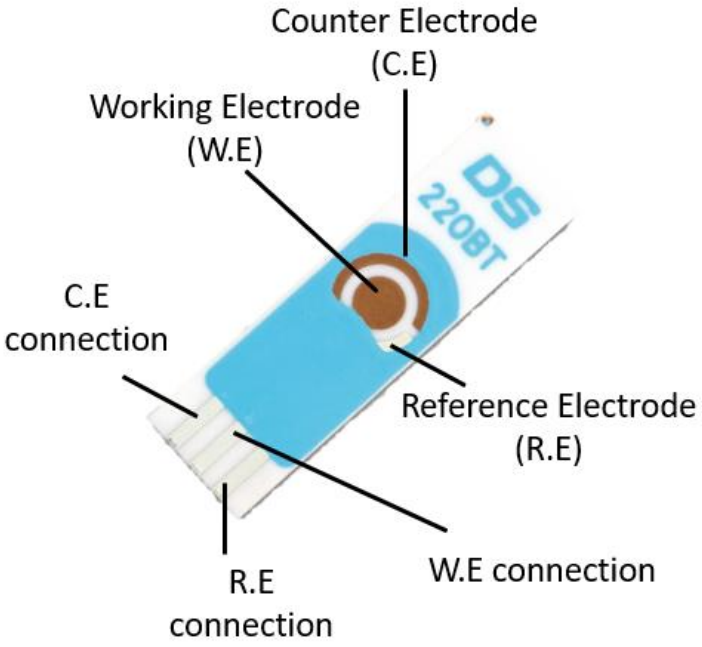

Figure 10 - Constitution of a SPE.

2.3. State of the Art for CRP biosensors

Up to now, there are already some biosensing systems proposed for the detection and quantification of CRP. In Table 1 are described some of the most recent biosensors. Most of the sensors described in the literature use antibodies as the biorecognition element. However, it is possible to observe that some aptamers and MIPs are already being developed.

In this work, Resende et al, [64] developed an immunosensor for the assessment of cardiovascular process using anti-reactive protein antibodies immobilized on a gold screen printed electrode. The authors obtained a linear range from 6.25 to 50 μg mL^{-1} and a detection limit of 0.78 μg mL^{-1}. The immunosensor developed for the detection of CRP using gold electrode showed efficacy and a potential use for the diagnosis and monitoring of cardiovascular disease progression.

In another study, Bryan et al, [65] presented a sensitive, label-free, non-amplified and reusable biochemical biosensor for the detection of CRP in blood serum, based on controlled and optimized immobilization of antibody coating on standard polycrystalline gold electrodes. The biosensor enabled a linear response over the concentration range of 0.5-50 nM and a LOD of 176 pM.

From a different perspective, Jarczewska et al. 2018, [66] applied an aptamer immobilization method on the gold surface and the content of the receptor layer was optimized to ensure efficient binding to the target protein. The quality of the monolayer was verified by applying chronocoulometry and atomic force microscopy (AFM). A linear response of the aptamer towards CRP was observed in the range of 1 to 100 pM.

In a different direction, Kumar et al,[67] developed a MIP with the biomimicking principle by incorporating 2-acryl amidoethyldihydrogen phosphate monomer that acts as if the natural phosphotidic choline binder in the synthesis of a novel printed polymer of CRP. The LOD was found to be 0.04 μg mL^{-1}.

In a recent research, Cui et al. 2022, [68] developed a highly sensitive protein MIP biosensor, in which conductive and biocompatible, antifouling nanosheets and specific MIPs were combined to achieve highly sensitive and selective recognition of human CRP. The authors used dopamine as a functional monomer to form a stable complex with the model molecule through hydrogen bonding and multipoint electrostatic attraction. The developed biosensor has a linear detection range of 10^{-5} to 10^{3} ng mL^{-1} and the LOD was found to be 0.41×10^{-5} ng mL^{-1}. The biosensor showed excellent selectivity, reversibility and reusability and long-term stability.

Table 1 - Some electrochemical biosensors reported in the literature.

Biorecognition Element	**Eletrochemical Detection**	**Linear Detection Range**	**LOD**	**Reference**
Antibody	EIS	0.5 to 50 nM	176 pM	[65]
Antibody	CV/EIS	50 ng mL^{-1} to 5 µg mL^{-1}	~90 pM or~11 ng mL^{-1}	[69]
Antibody	EIS	100 ng mL^{-1} to fg mL^{-1}	1 fg mL^{-1}	[70]
Antibody	Amperometry	2 to 100 µg mL^{-1}	0.80 µg mL^{-1}	[71]
Antibody	Amperometry	1 to100 µg mL^{-1}	0.54 µg mL^{-1}	[72]
Antibody	EIS	6.25 to 50 µg mL^{-1}	0.78 µg mL^{-1}	[64]
Antibody	EIS	1 to 1000 ng mL^{-1}	0.08 ng mL^{-1}	[73]
Antibody	EIS/CV	10 to 160 nM	37 nM	[74]

Aptamer	CV	1 to 100 pM L^{-1}	25.9 pMl L^{-1}	[75]
Aptamer	SWV	1 to 100 pM	1 pM	[66]
MIP	CV	0.18 to 8.51 μg mL^{-1}	0.04 μg mL^{-1}	[67]
MIP	EIS	10−5 to 103 ng mL^{-1}	10 ng mL^{-1}	[68]
MIP	SWV	0.1 nM to 500 nM	0.1 nM	[76]
MIP	CV	0.01 pM to 1 μM	0.01 pM	[77]

Although great achievements have been accomplished regarding innovative biosensing platforms for CRP detection, the introduction of chitosan biopolymeric material into the assembly of the biosensor is herein proposed to improve biocompatibility and stability performance. Choosing the appropriate monomer is crucial as its functional groups will interact with specific sites on the protein, facilitating a more tailored molecular imprinting process. Therefore, aniline was selected as the electropolymerizable monomer for the construction of the MIP onto Au-SPE. Aniline contains amino groups that can interact with gold surfaces through chemisorption or the formation of self-assembled monolayers, ensuring a strong and stable attachment to the electrode. Furthermore, aniline exhibits excellent electrochemical properties, making it suitable for the electropolymerizing process and ensuring the generation of a durable and efficient biosensor for the detection of analytes [78]. Innovation at this level can be accomplished by the integration of chitosan, a biocompatible and biodegradable material derived from natural sources, such as shellfish shells. It possesses antimicrobial properties, is non-toxic, and has low immunogenicity, making it suitable for biomedical applications. Chitosan has been widely investigated for various medical purposes, including wound healing, drug delivery systems, and tissue engineering, due to its favorable properties [79]. In most of the cases, chitosan has been incorporated in the assembly of biosensors as a suitable substrate for immobilizing biomolecules or as a protective coating, however, herein this adhesive and biocompatible material will be integrated in the polymeric matrix of the sensing device [80].

3. METHODS

In this chapter, a comprehensive description is provided regarding the reagents, materials, equipment's, and experimental procedures employed for the development and optimization process of the CRP electrochemical biosensor.

3.1. Reagents, Materials and Equipments

For the preparation of solutions, adjustable volume micropipettes from the Eppendorf brand were used (2-20 µl, 20-200 µl, 100-1000 µl, and 1000-5000 µl). Regarding the weighing of reagents, a Mettler Toledo balance (model MS105DU with a precision of ± 0.0001g) was employed. Solutions were prepared in Class A volumetric flasks with capacities of 10 mL and 500 mL. Additionally, for solutions that were difficult to dissolve, a low surface tension liquid agitator from Fisherbrand was used. Along the experiments, the pH meter was the GLP 21 model from CRISON, and the SELECTA ultrasonic device was employed for the homogenization of various solutions.

Table 2 details all reagents used in the development of this work, as well as their commercial origin.

Table 2 - List of reagents used.

Reagent	**Commercial Origin**
Acetic Acid (CH_3COOH)	Carlo Erba
Aniline (C_6H_7N)	Sigma Aldrich
Chitosan (Degree of deacetylation ≥ 75%)	Thermo Scientific
C-Reactive Protein	Merck
Glucose monohydrate ($C_6H_{12}O_6{\cdot}H_2O$)	Alfa Aesar
Immunoglobulin G (IgG)	Sigma Aldrich
Methanol (CH_3OH)	Riedel-de-Haen
Potassium hexacyanoferrate (II) ($K_4[Fe(CN)_6]$)	Riedel-de-Haen
Potassium hexacyanoferrate (III) ($K_3[Fe(CN)_6]$)	Riedel-de-Haen
Protein IL-6	abcam
Sodium Acetate ($CH_3COONa.{}_3H_2O$)	Riedel-de-Haen
Sulphuric Acid (H_2SO_4)	Sigma Aldrich

Electrochemical measurements were applied using a Metrohm Autolab potentiostat (Figure 11), controlled by Nova 1.11 software, and a Metrohm DropSens connector box (DRP-DSC) (Figure 12), interfaced with the Autolab device.

The conductive gold SPEs used were acquired from Metrohm DropSens and consisted of:

- Ceramic substrate
- Dimensions: 3.4 x 1.0 x 0.05 cm
- Electrical contacts: Gold working electrode (4 mm diameter), gold/ platinum counter electrode, and silver reference electrode.

Figure 11 - Metrohm Autolab potentiostat.

Figure 12 - Metrohm DropSens connector box (DRP-DSC).

3.1.1. Solution preparation

In the experimental procedures, ultrapure water obtained from the Milli-Q system was utilized for the preparation of solutions, ensuring high purity, and minimizing potential contaminants. Specifically, Acetate Buffer solution was prepared with a final concentration of 0.25 mM and maintained at a pH of approximately 6.

To perform the electrochemical measurements, a redox standard solution was employed, comprising potassium hexacyanoferrate (II) and potassium hexacyanoferrate (III) at concentrations of 5.0 mM each. These standard solutions were prepared in Acetate Buffer to maintain stability and provide a suitable environment for the electrochemical reactions. The sulfuric acid and acetic acid solutions were prepared in ultrapure water, with a concentration of 0.5 M and 0.1 M, respectively.

The 1% chitosan solution was prepared in 0.1 M acetic acid. Aniline was diluted in Acetate buffer to a final concentration of 5 mM.

CRP was diluted in Acetate buffer solution to achieve a concentration of 100 μg mL^{-1} (stock). In order to construct the calibration curve, a series of standard solutions were prepared by successive dilutions, starting with the CRP stock solution to a concentration of 0.001 ng mL^{-1} and using the same buffer. This resulted in the generation of seven standard solutions. The schematic representation of this procedure is depicted in Figure 13.

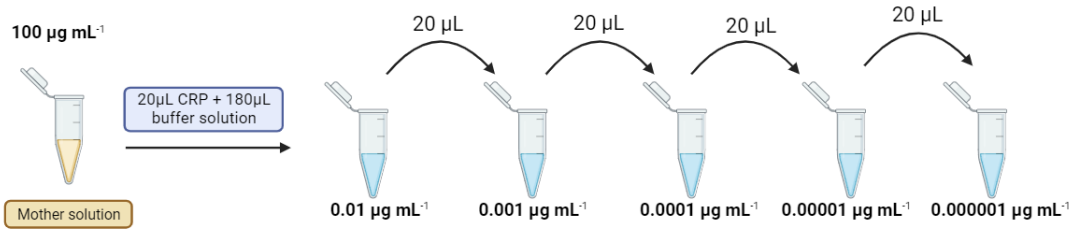

Figure 13- Illustrative scheme for the preparation of different standards by consecutive dilutions of the concentrated CRP stock solution.

3.2. Sensor fabrication

In order to assembly a MIP-based sensor for CRP molecule, a mixture containing chitosan and aniline was prepared, in the presence of CRP. The preparation and construction of the biosensor involved three essential steps: (i) electrochemical treatment of the gold surface, (ii) electropolymerization process, and (iii) removal of the protein to create the specific cavities. The response of the biosensor was assessed through a series of repeated incubations with the target protein, evaluating its re-binding capabilities. The construction process of the MIP in this study is illustrated in Figure 14.

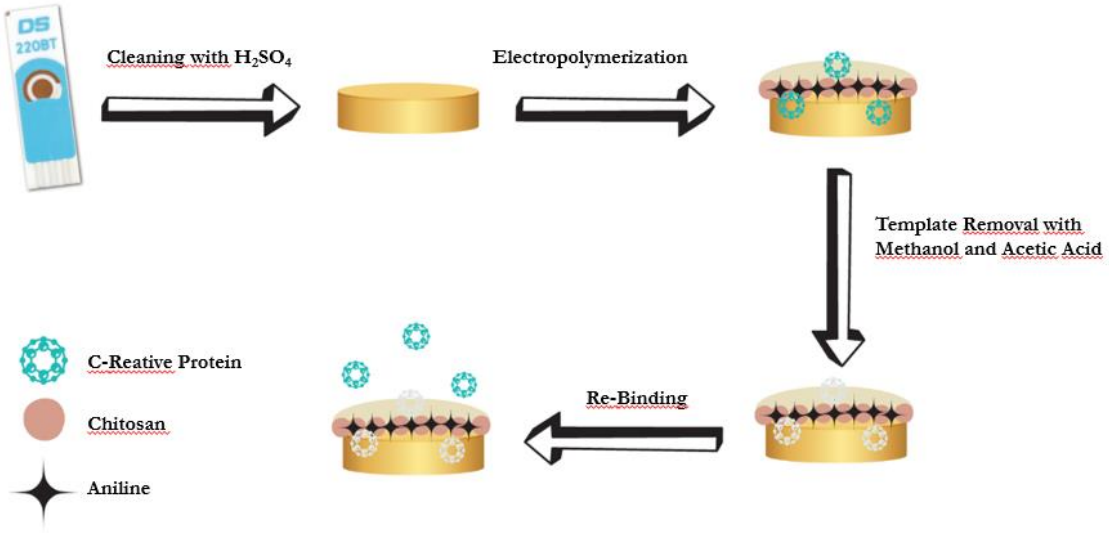

Figure 14- Schematic illustrating the different steps in the construction of a MIP-based electrochemical biosensor for the detection of CRP.

The modifications made to the electrodes were assessed after each step using the redox probe solution (90 µL) and the EIS electrochemical techniques. EIS readings were obtained at an open-circuit potential after 60 seconds, covering a frequency range from 1 to 100000 kHz, with 50 frequency values and an amplitude of 0.01 V.

Following the electropolymerization technique, where the MIP was synthesized, measurements with the redox probe solution were exclusively carried out using the EIS technique. This decision was based on

the stability of the aniline and involved a frequency range of 0.1 to 100000 kHz to capture the complete charge transfer resistance.

3.2.1. Electrochemical treatment

Along the biosensor construction, the initial step involves performing electrochemical cleaning/ treatment to the electrode surface, which plays a crucial role in eliminating any potential impurities and contaminants present on the surface of the Au-SPE. This process is considered essential to ensure a clean substrate for subsequent modifications, as well as for reproducibility issues.

Additionally, the electrochemical cleaning step promotes the activation of functional groups on the surface of the WE, facilitating the formation of a polymeric matrix. This activated surface enables the binding and interaction of the protein with the surface, facilitating the desired biosensing capabilities of the device. For the cleaning process, a 0.5 mM solution of H_2SO_4 was employed. CV was employed as the electrochemical technique, with measurements conducted by scanning the potential range from -0.2 V to +1.2 V. The scan was repeated for 5 cycles at a scan rate of 0.05 V s^{-1}.

3.2.2. Electropolymerization conditions

Electropolymerization plays a crucial role in MIP synthesis of this study. It is a pivotal step in creating a polymeric matrix, which forms an ultra-thin film on the surface of the WE. This matrix serves to interact with and bind the target compound, leading to the creation of cavities that mimic the shape and properties of the target molecule once the target molecule is removed.

Regarding the electrochemical polymerization, some experimental parameters were studied:

- The effect of chitosan presence during aniline electropolymerization (1:1 mixture)

A study was conducted to test the stability of the biosensor without the addition of chitosan.

- Scan-rate during electropolymerization

In this study, one of the factors investigated was the scanning speed employed during the electropolymerization process. This parameter plays a significant role in determining the growth characteristics of the polymer on the electrode surface, potentially resulting in either denser or more porous polymeric structures. To explore the effect of different scan-rates, a mixture of chitosan-aniline was used. Specifically, 90 µL of the solution was applied to the electrodes and subjected to CV over a potential range of -0.6 V to +1.0 V for 5 cycles. Three different scanning speeds were tested: 0.020 V s^{-1}, 0.050 V s^{-1}, and 0.1 V s^{-1}.

- Number of cycles during electropolymerization

The electrodes were covered with a solution containing aniline and chitosan, which underwent polymerization through CV within a potential range of -0.6 V to +1.0 V, utilizing a scan rate of 0.05 V s^{-1}. Lastly, the study assessed the influence of varying polymerization cycles, specifically analyzing the outcomes of 3, 4, and 5 cycles, respectively.

- CRP concentration

The CRP concentration plays a vital role in determining the biosensor's response during MIP preparation. It influences the abundance of (bio)recognition points, thereby affecting the overall outcome. To investigate this, a study was conducted using a concentration ten times lower than the one employed for analyzing the sensor's response (5 µg mL^{-1} and 0.5 µg mL^{-1}).

3.2.3. Template Removal

After electropolymerization, the challenging task of protein removal is undertaken, which is a crucial step in the molecular imprinting technique. The primary objective of this step is to remove the template protein from the previously formed polymer matrix. However, the challenge lies in the fact that the removal agent inevitably affects the polymer matrix. Hence, it becomes imperative to compare NIP with the MIP since the goal is to minimize or avoid any alterations caused by the removal agent on the NIP. Any changes observed on the surface of NIP can be attributed either to the adsorption of the removal agent on the sensor surface or to potential damage induced to the polymer matrix itself.

To undergo this study, the effect of different removal agents was tested, like (1) a mixture of acetic acid with methanol, (2) an ethanolic diluted solution, and acetone.

Table 3 shows the procedure performed with the different removal agents.

Table 3 - List of removal reagents used and their practical procedure.

Removal agent	**Description of the procedure**
Methanol and Acetic acid	Incubation of the 4:1 mixture for 5 min, followed by incubation for 30 min in acetate buffer
Acetone	Incubation of acetone for 10 min, followed by incubation for 30 min in acetate buffer
Ethanol diluted in ultrapure water	Incubation of the 1:1 mixture for 3 hours, followed by incubation for 30 min in acetate buffer
Ethanol diluted in ultrapure water	Incubation of the 1:1 mixture overnight, followed by incubation for 30 min in acetate buffer

Following the careful selection of the removal method, a subsequent investigation was conducted to determine the optimal removal time. Specifically, using the removal agent consisting of methanol with acetic acid, removal times of 5 and 15, minutes were systematically tested and evaluated.

3.2.4. Calibration curve

After optimizing the biosensor construction process, the subsequent phase focused on evaluating its capability to detect the target protein, CRP. This assessment involved determining the biosensor's capacity to interact with and reestablish connections with the protein through the mold cavities created during its removal.

In order to construct the calibration curves, the biosensor underwent an incubation process in buffer solution. This involved successive incubations of 5 µl of the blank solution (Acetate Buffer) on the WE surface for 30 minutes, followed by a reading with the redox probe solution after each incubation. Once the signal was stabilized, incubations with standards (as listed in Table 4) were performed. Each standard, with a volume of 5 µl, was incubated on the WE surface for 30 minutes, followed by a reading of EIS with the redox solution after each incubation.

In summary, the calibration curves were generated using the electrochemical EIS technique. A series of data points obtained through readings with the redox solution, varying according to the concentration of the analyte, were utilized to construct these curves. This approach facilitated the establishment of a relationship between the signal intensity and the concentration of the CRP.

Table 4 - Set of CRP standard solutions diluted in Acetate Buffer and their concentration.

Standard Solution	CRP concentration (μg mL^{-1})
1	0.000001
2	0.00001
3	0.0001
4	0.001
5	0.01
6	0.1
7	1

3.2.5. Selectivity Study

During the assessment of the analytical performance of a biosensor, it is crucial to not only evaluate its ability to detect the target analyte across various concentrations but also to ensure its selectivity towards the biomolecule. This is particularly significant when considering the potential application of the biosensor in clinical tests, where it will encounter complex fluid samples such as cell extracts, blood, urine, wound fluids and serum. Thus, one of the primary objectives of biosensors is to accurately identify the analyte within such a complex environment, highlighting the importance of its selective response to the specific analyte of interest.

In this phase of the research, a selectivity study was conducted using IL-6 protein (C=0.0001 μg mL^{-1}), immunoglobulin G (IgG) antibody (C=0.0001 μg mL^{-1}) and Glucose (C=0.0001 μg mL^{-1}) as interferent molecules. To prepare the interferent solutions, IgG and Glucose were accurately weighed and diluted in acetate buffer to achieve the desired final concentration. For IL-6, successive dilutions were carried out in acetate buffer until a final concentration of 0.0001 μg mL^{-1} was attained. Following this, each interferent solution was mixed with a CRP solution (0.0001 μg mL^{-1}).

To carry out the experimental procedure, the selectivity study was performed only with MIP-based sensors. Before incubation with the mixture CRP+Interferent, each sensor underwent stabilization in Acetate buffer for 30 minutes. Subsequently, a reading using the EIS technique was taken using the redox probe solution to evaluate the response. All experiments were performed in triplicated.

3.3. Characterisation Study

In order to follow each modification occurring on the surface of the Au-SPEs, Scanning Electron Microscopy (SEM), Fourier Transform Infrared Spectroscopy (FTIR) and Raman techniques were employed.

SEM analysis was conducted using FEI Quanta 400FEG ESEM/EDAX PEGASUS X4M equipment. SEM analysis was performed externally by CEMUP group, University of Porto and was performed at an accelerating voltage of 25 kV. For the SEM analysis, the polymeric films were grown on Au-SPE for 5 CV cycles.

FTIR was performed using a Thermo Scientific iTR Nicolet iS100 spectrometer coupled to an attenuated total reflectance (ATR) sensor with germanium (GE) contact crystal. Both sample and background spectra were acquired under the control of room temperature and humidity with 90 scans and a resolution of 16 cm^{-1} in the spectral range from 700 to 4000 cm^{-1}.

The Raman spectra were obtained using a Thermo Scientific DXR Raman microscope system. A 785 nm excitation laser was utilized, and the specific parameters employed can be found in Table 5.

Due to the small amount of polymeric material available on the top of the electrodes for the FITR and Raman analysis, polymeric films were grown on Au-SPE for 10 CV cycles. Before measurement, the samples were left to dry at room temperature for at least one day.

Table 5 - List of parameters and their configuration for obtaining Raman spectra.

Parameters	**Configuration**
Potential	785 nm
Aperture	50 μm slit
Photo-bleach	1 min
Exposure time	5 seg
Enlargement	50 x

4. RESULTS AND DISCUSSION

In the development process of the electrochemical biosensor for the detection of CRP, several optimizations were performed along the different construction steps previously mentioned in chapter 3. Thus, the aim of chapter 4 is to describe, present and discuss the different optimization results that led to the final design of the proposed biosensor.

4.1. Construction and optimization of the biosensor

As previously mentioned, the mixture selected for the development of this biosensor is composed of the monomer aniline (Figure 15 a) with the polymer chitosan (Figure 15 b). Aniline monomers are transformed into a polymer called polyaniline by the process of aniline polymerization. Aniline can be polymerized in a variety of ways like chemical oxidative polymerization [81], electrochemical polymerization [82], enzymatic polymerization [83] and photochemical polymerization [84]), although chemical oxidation is the most typical process [85], [86]. The process of polymerizing aniline typically involves oxidative coupling, in which the monomers of aniline are subjected to a series of oxidation and coupling reactions to create a long-chain polymer with repeating units [85], [87]. The electrochemical technique known as CV is frequently used to examine the redox behavior of the produced conductive polymer polyaniline. As aniline polymerizes, the redox characteristics of the polymer change as a result, producing distinctive peaks in the cyclic voltammogram. The redox reactions that take place during the electrochemical oxidation and reduction of the polymer can be identified by the different peaks obtained during the CV of aniline polymerization [85], [86].

a) b)

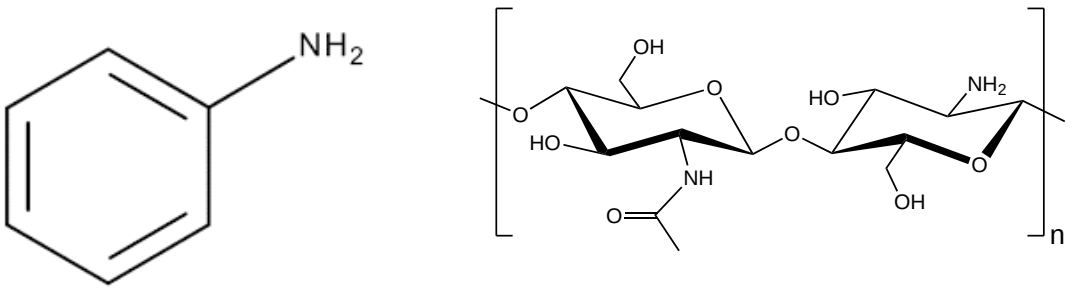

Figure 15 - Structure of a) aniline [88] and b) chitosan [89].

In this work, the biopolymer chitosan was incorporated in the matrix during the electropolymerization of aniline monomer. Chitosan is a naturally occurring biopolymer obtained from chitin deacetylation, which is present in the cell walls of fungus and the exoskeletons of crustaceans [79]. When mixed with aniline and electropolymerized, the resultant co-polymer has special characteristics and functions that are advantageous for many applications, such as biomedical applications, biosensors, and wound healing [80], [90]. Biopolymer chitosan is an intriguing option for sustainable chemistry and engineering since it also promotes sustainability and lessens environmental effect [79], [80]. More specifically the adhesive properties of chitosan make it very appealing for application in wound healing. Its composition includes amine groups, which makes it even more interesting because they give chitosan its cationic polymeric character [91]. When utilized in biomedical applications, this positive charge enhances interaction with biological tissues, cells, and proteins, making it biocompatible and minimizing unfavorable effects. Because the amine functional groups are reactive, chitosan can take part in a variety of chemical processes. Chitosan is extremely changeable due to its activity, making it feasible to add other groups or

molecules to its structure to get specific functional qualities. Chitosan can be used in the creation of controlled medication release systems in order to preserve pharmaceuticals from acidic conditions and release them at specified locations inside the body [91]. Chitosan is still widely used for functionalizing and modifying surfaces however there are still very few works on the construction of MIPs.

Taking account all the aforementioned advantages of chitosan, it was essential to evaluate the different behavior of the polymer sensor matrix with and without the presence of chitosan during the development of the biosensor.

Figure 16 shows (a) the cyclic voltammograms regarding the electrochemical polymerization reaction as well as (b) the Nyquist plots obtained after the electropolymerization of aniline alone and in the presence of chitosan.

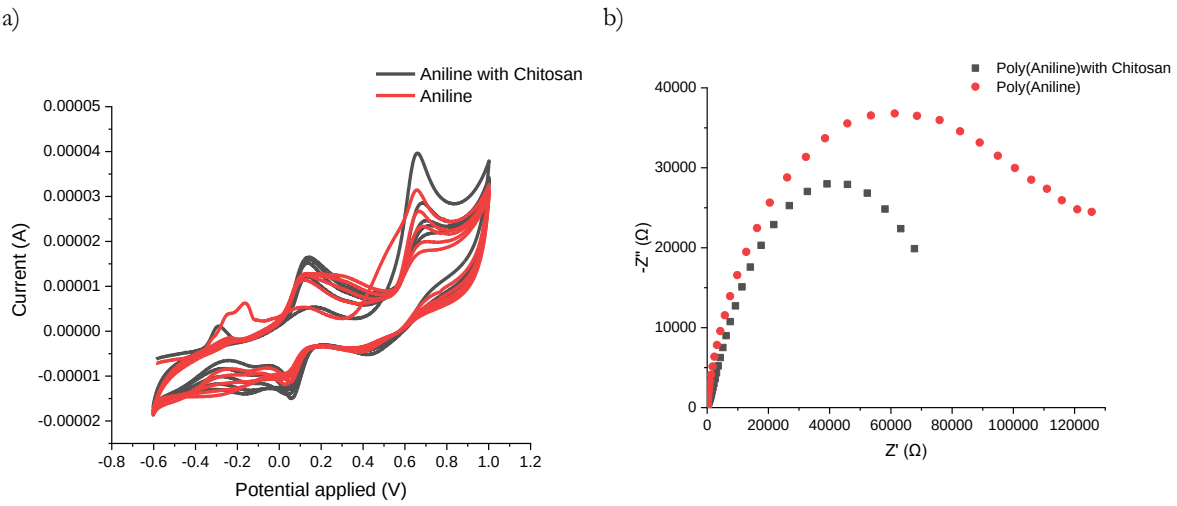

Figure 16 – a) Cyclic voltammograms during electropolymerization of aniline with and without the addition of chitosan; b) Nyquist plots obtained after electropolymerization of aniline alone and with chitosan.

As can be seen from Figure 16 a), the peaks obtained during the electropolymerization of aniline alone and with chitosan are very similar. The peak shown at +0.8 V represents the aniline oxidation peak [92].

Along this investigation, the construction of NIP and MIP sensors was followed in-situ by EIS measurements in 5 mM $[Fe(CN)_6]^{3-/4-}$ solution, prepared in 0.25 M acetate buffer as the supporting electrolyte. EIS was employed as a non-invasive technique since it holds the advantage of not causing any damage or disturbance to the modified surface of the electrochemical system. Looking to Figure 16 b), it can be seen that poly(aniline) alone exhibits a greater Rct in comparison to the polymeric film with chitosan, as can be observed from the Nyquist plots and, as expected, it was necessary to conduct more electrochemical readings until it becomes stabilized.

4.1.1. Optimization of electropolymerization parameters

Various methods can be explored during the production of MIP-based materials to achieve optimal detection features such as sensitivity, reproducibility, and detection limits.

In this study, the bulk imprinting approach was selected which enabled one-single step of electropolymerization in the presence of the target molecule. One of the main issues that should be taken

in consideration during this type of imprinting concerns the affinity between the monomers and the molecule to be imprinted.

Finding the ideal pH for dealing with a specific protein is a crucial consideration before moving further with the imprinting process. The pH of 6.0 was used for the experiment. Firstly, this pH was chosen due to chitosan's insolubility in neutral and alkaline environments. Moreover, above their isoelectric point (Ip), (CRP Ip is about 5.2) [93], proteins deprotonate and are mostly negatively, making them more favorable to interact with the positively charged amine groups present in chitosan.

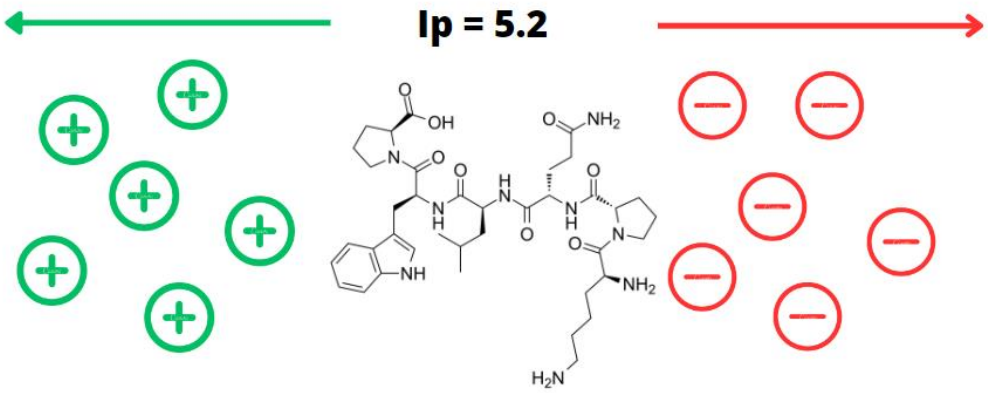

Figure 17 - Schematic of charge distribution for CRP structure according to pH variation.

The first study to be performed was the optimization of the scanning rate. The scanning speed during the electropolymerization step directly influences the growth and porosity of the polymeric matrix, i.e., the higher the scanning speed, the greater the porosity of the formed polymeric film [94], [95]. Three different scanning speeds (0.02 Vs^{-1}, 0.05 Vs^{-1}, 0.1 Vs^{-1}) were tested. Figure 18 a), b), c) shows the EIS results of the electrochemical measurements with the redox probe solution after each polymerization regarding the NIP and MIP sensors for the different scanning speeds.

a)

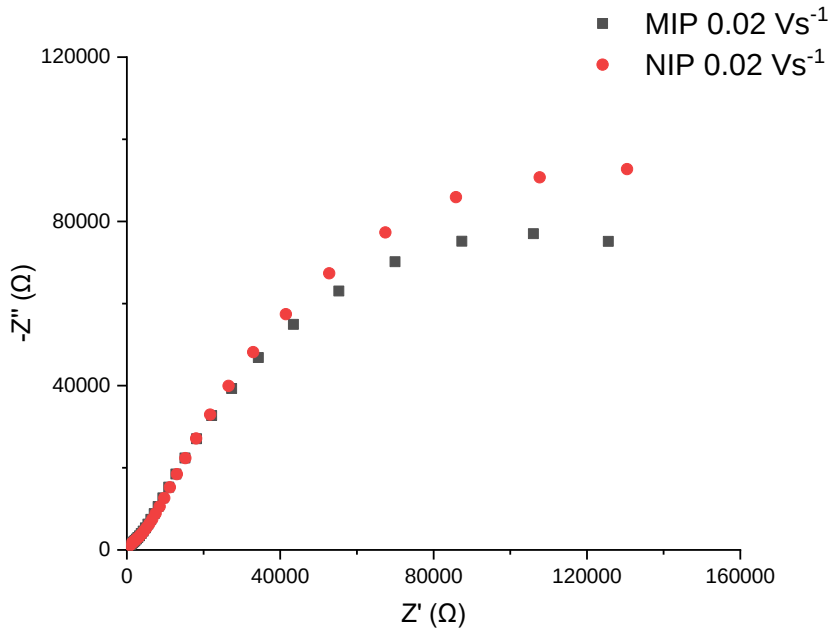
MIP 0.02 Vs-1
NIP 0.02 Vs-1
120000
80000
40000
0
-Z'' (Ω)
0
40000
80000
120000
160000
Z' (Ω)

b)

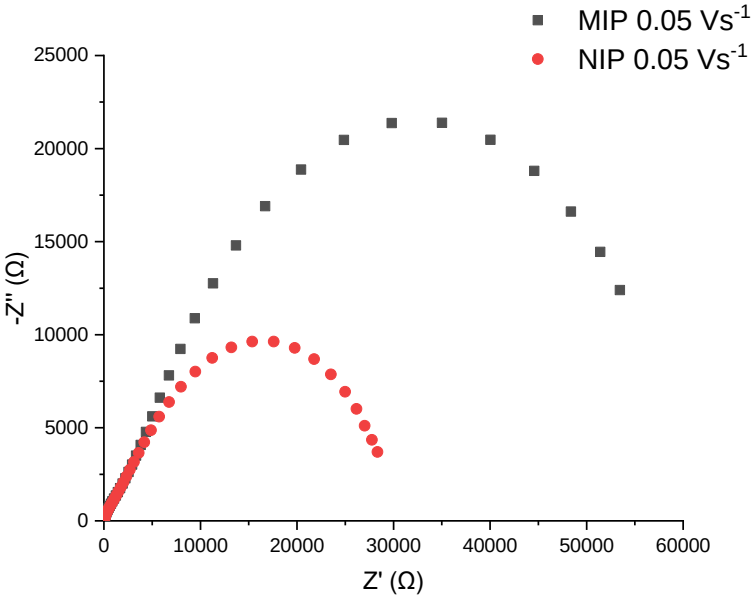
MIP 0.05 Vs-1
NIP 0.05 Vs-1
25000
20000
15000
10000
5000
0
-Z'' (Ω)
0
10000
20000
30000
40000
50000
60000
Z' (Ω)

c)

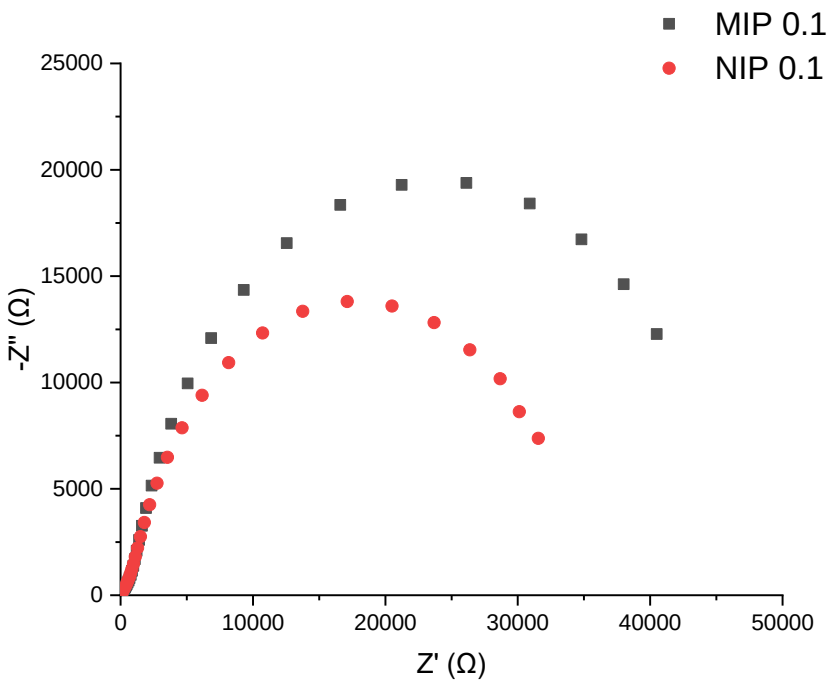

Figure 18- Nyquist plots obtained for NIP and MIP fabrication with a scan rate of a) 0.02 Vs^{-1} ; b) 0.05 Vs^{-1}; c) 0.1 Vs^{-1}.

From the profiles obtained, for the scanning speed at 0.02 Vs^{-1} (Figure 18 a)) there is a significant increase in the resistance to the passage of current in comparison to the other higher scanning speeds. This is explained by the porosity of the polymer matrix, i.e., the higher the scanning speed, the larger the diameter of the pores formed by electropolymerisation and the lower the Rct observed. Higher scanning speeds produce polymers less crosslinked, which can make molecular imprinting challenging because their pores can be larger than the biomolecules' diameter. Additionally, because the polymer layer is too large, the molecules may not have enough force for release and leave their cavities during the template removal step. Furthermore, the Rct between MIP and NIP was shown to differ significantly more at the scan rate of 0.05Vs^{-1} than for the other scan rates examined. This may be a strong indication that more protein was entrapped at this scan-rate condition. Thus, Figure 19 shows the calibration curves obtained regarding the MIPs fabricated at the different scan-rates tested.

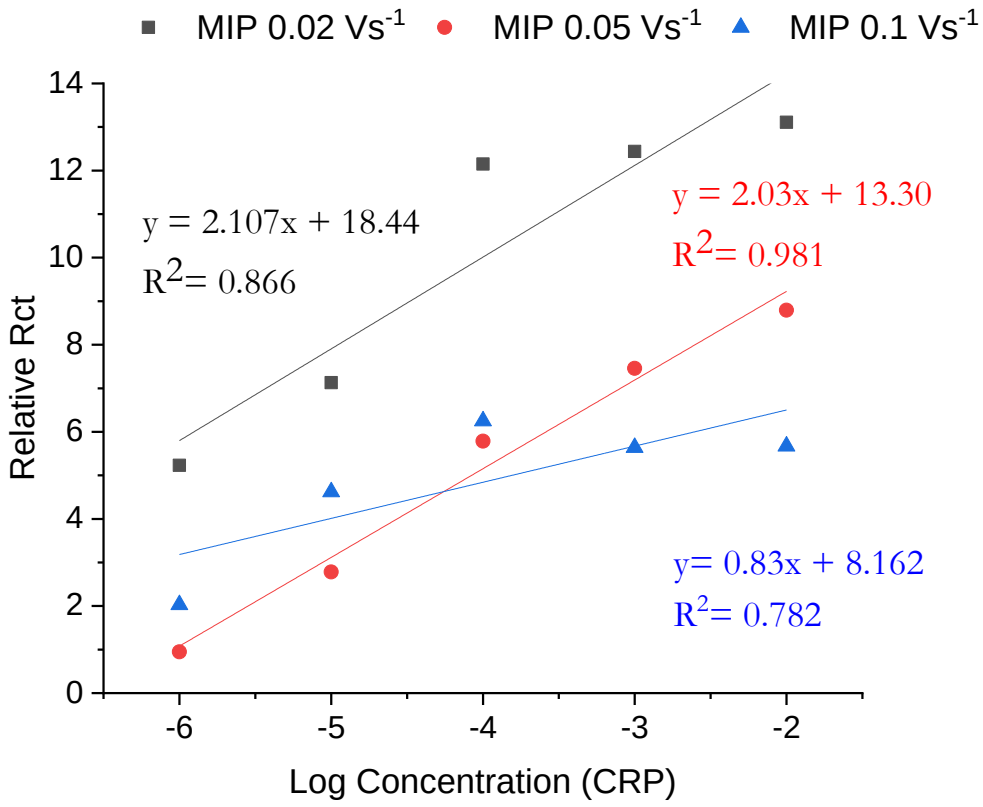

Figure 19 - Calibration curves obtained for MIP sensors fabricated at different scan rates (0.02 Vs^{-1}, 0.05 Vs^{-1}, 0.1 Vs^{-1}).

Having said that, analyzing the graphs of the calibration curves (Figure 19) it is possible to see that the scanning speed of 0.05 Vs^{-1} was undoubtedly the one that led to the best performance of the biosensor, presenting a good linearity correlation (R^2=0.981). In the case of 0.1 Vs^{-1} there is no linear correlation, since it presented a completely random result in the calibration, without linearity (R^2=0.782). This may be due to the fact that higher scan rates lead to faster reactions, less polymer crosslinking, potentially resulting in less uniform and stabilized cavities. This can affect the reproducibility and quality of the resulting polymer [96].

Furthermore, in the case of the 0.02 Vs^{-1} scan rate, it is possible to draw a straight line (R^2=0.866) however it is not a linear response as in the 0.05 Vs^{-1} scan rate. Therefore, it is concluded that at 0.02 Vs^{-1} molecular imprinting may not have occurred due to the matrix being a very dense polymer, or since the polymer matrix is so dense, protein removal may not have been effective.

Figure 20 shows the CVs of MIP and NIP electropolymerization at the best condition obtained with scanning speed of 0.05Vs^{-1}.

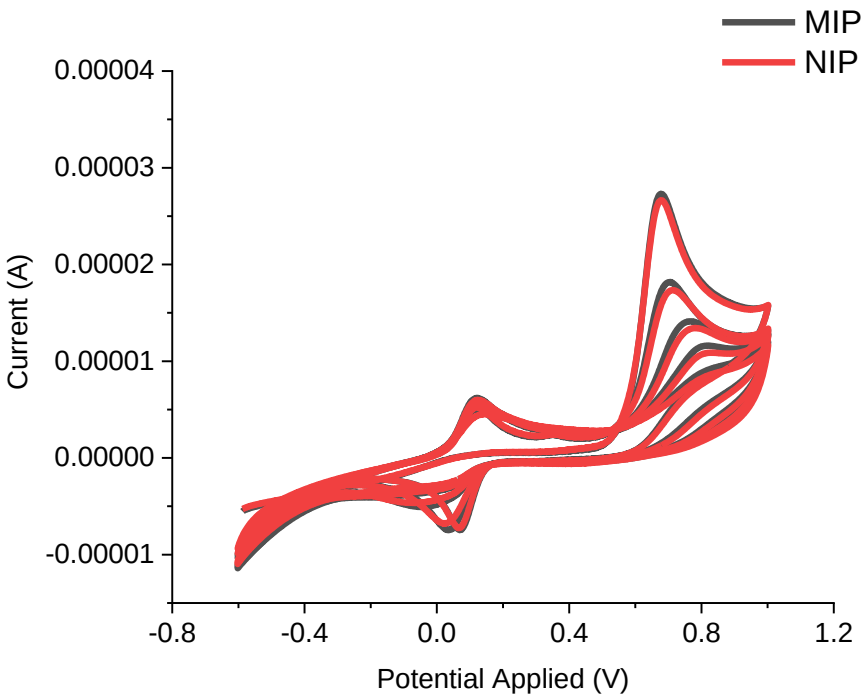

Figure 20 - Cyclic voltammograms regarding NIP and MIP sensors obtained after electropolymerization at a scanning speed of 0.05 Vs^{-1}.

From the graph presented, it can be analyzed that there are no significant differences between the cyclic voltammograms of the MIP and the NIP. Both show a very prominent aniline oxidation peak (+0.8 V). They also present two peaks at +0.2 V and +0.3 V which are believed to be oxidation and reduction of traces of the redox probe solution from previous readings, since the signal attenuates with increasing cycles.

After selecting the most suitable scanning speed for electropolymerization, the effect of the number of cycles during electropolymerization was investigated. When growing the polymer around the protein template, precise control of the film thickness is crucial, particularly for MIPs based on bulk imprinting, to avoid complete entrapment of the protein.

Figure 21 shows the results of the electrochemical readings obtained after electropolymerization of NIPs performed at different numbers of cycles.

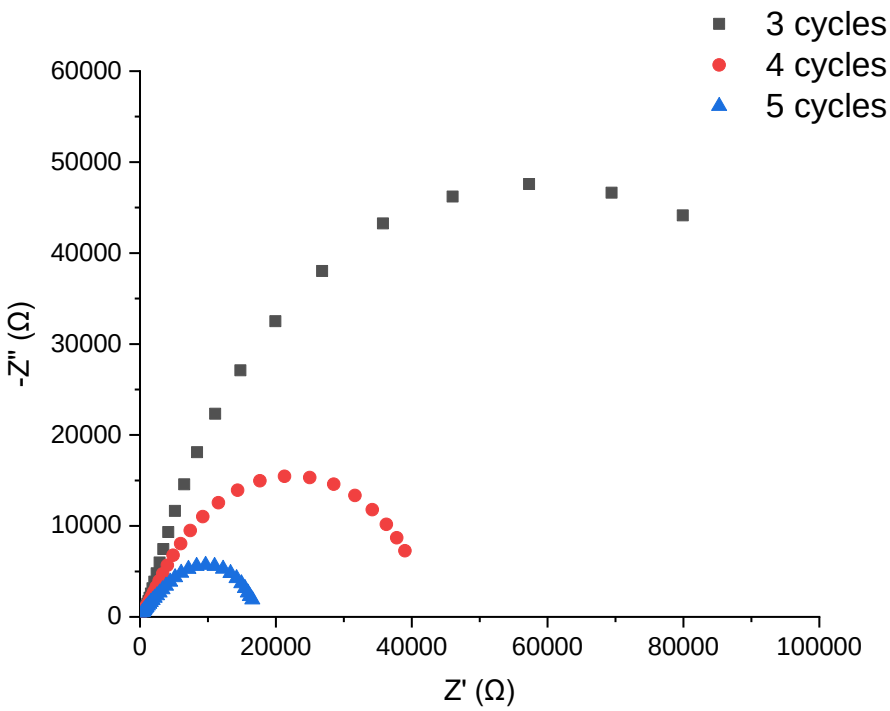

Figure 21 - Nyquist plots after 3, 4 and 5 cycles of NIP electropolymerization.

All the electrodes used in the investigation showed unambiguously noticeable increases in Rct values following the electropolymerization procedure.

It was observed that increasing the polymerization cycles from 3 until 5 resulted in lower Rct values which can be explained due to the conductivity behaviour of poly(aniline) in acidic conditions [97]. Poly(aniline) is conductive in an acidic medium, so when it is electropolymerised for more cycles, the formed poly(aniline) can become more conductive and present a lower Rct than when electropolymerisation occurs with fewer cycles [67], [77] . Moreover, a higher number than 5 cycles was not tested since it could entrap the CRP protein and buried deep within the polymeric film.

4.1.2. Effect of removal agents on the polymer matrix

One important issue that will define biosensor's performance regards the type of removal agent because it will be responsible to create MIP sensors with well-defined and complementary cavities, without causing harm to the polymer matrix.

Therefore, under ideal circumstances, the removal agent should encourage a change in the MIP signal and should essentially maintain the NIP signal intact, indicating that the protein has been removed without risk of adsorption to the surface or damage to the polymer matrix. Thus, different removal agents such as methanol with acetic acid, acetone, ethanol with ultrapure water were tested.

In order to evaluate the effect of the different removal agents, incubation assays were performed in the sensor area and afterwards, electrochemical readings were conducted to assess the alterations of the surface during the removal treatment. Figure 22 concerns the MIP data corresponding to the percentage variation regarding Rct values for each of the different removal agents.

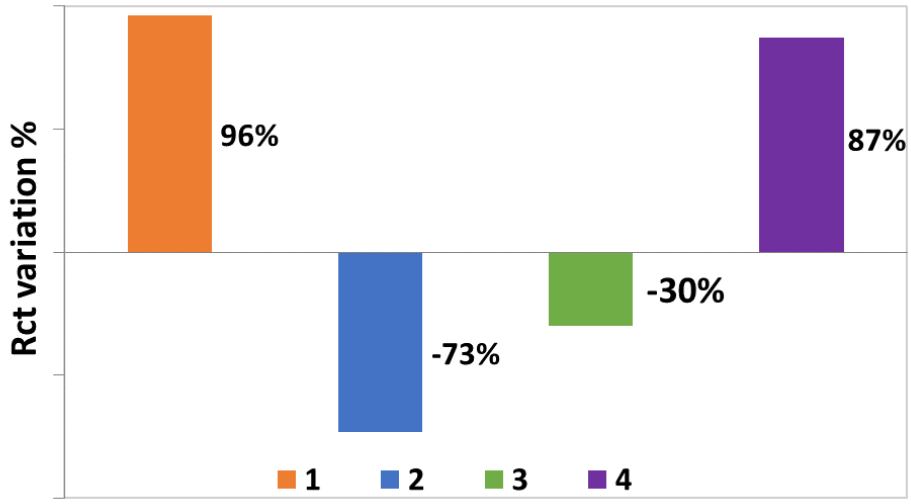

Figure 22 - Bar chat corresponding to the percentage removal of the MIPs: 1)- 4:1 Misture of methanol with acetic acid; 2)- 1:1 Mixture of ethanol with ultrapure water for 3h; 3)- 1:!1 Mixture of ethanol with ultrapure water overnight; 4)- Acetone.

The complete eradication of the imprinted protein from MIPs would be the primary goal of the removal. Unfortunately, even after numerous wash cycles, it is still challenging to completely remove the mold. This is primarily because highly crosslinked sections are difficult to reach by solvents or the mold is not soluble enough in the solvent to disrupt interactions with the printed cavities [98].

As can be seen in Figure 22, employing ethanol combined with ultrapure water as the removal agent, caused an increase of the Rct value, as opposed to the other removal agents (mixture of methanol with acetic acid and acetone). As mentioned before, the use of different removal agents can alter the morphology of the MIP, which could explain this change in polymer shape. In addition, the microstructure and organization of the polymer can be impacted by the presence of the mold during polymerization, which can change the polymer's electrical characteristics. This well-organized structure may be disturbed by mold removal, which could hold a great impact in its resistance [98].

Furthermore, it can be seen that the mixture of methanol and acetic acid was the removal approach that enabled a higher variation in the imprinted sensor (96% removal percentage), with a substantial Rct decrease of the MIP film, as the result of the formation of imprinted cavities that
facilitate the diffusion of $Fe(CN)_6^{3-/4-}$ through the polymer network Afterwards, the best removal time was also optimized. As a result, two different removal times - 5 minutes and 15 minutes - were investigated. Figure 23 shows the Nyquist plots obtained for the MIPs treated with different time of removal incubation before and after model removal and the corresponding calibration curves.

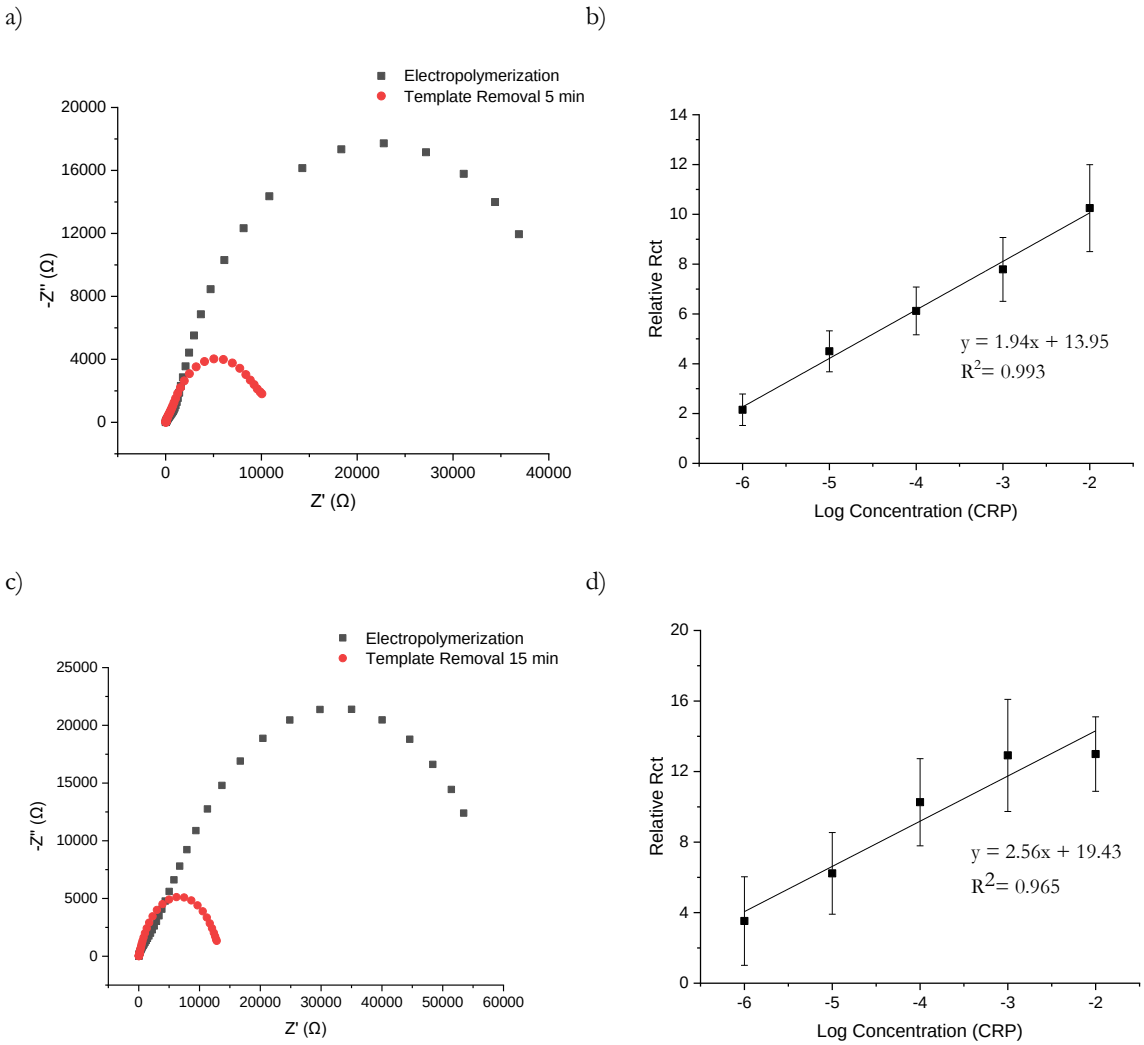

Figure 23 - a) Nyquist plots for MIP before and after template removal for 5 min; b) MIP calibration curves with 5 min of template removal; a) Nyquist plots for MIP before and after template removal for 15 min; b) MIP calibration curves with 15 min of template removal.

Although EIS data did not display substantial differences for 5 (removal percentage of approximately 90%) and 15 min (removal percentage of approximately 80%) of removal, the calibration curves showed that 5 minutes yields the greatest result in terms of linearity and reproducibility.

Less removal time may have produced better results because when the polymer is in contact with the removal agent for an extended period, the polymeric film may begin to deteriorate or change rather than leaving the imprint sites open for analyte identification [98].

Excellent linearity was seen during the calibration of the MIP at a 5-minute removal condition. Additionally, compared to the MIP with 15 min removal (R^2 of 0.965), the MIP with 5 min removal showed good sensitivity and higher linear correlation (R^2 of 0.993).

In sum, after the previously discussed optimization conditions, the EIS results regarding the NIP and MIP assembly are shown in Figure 24.

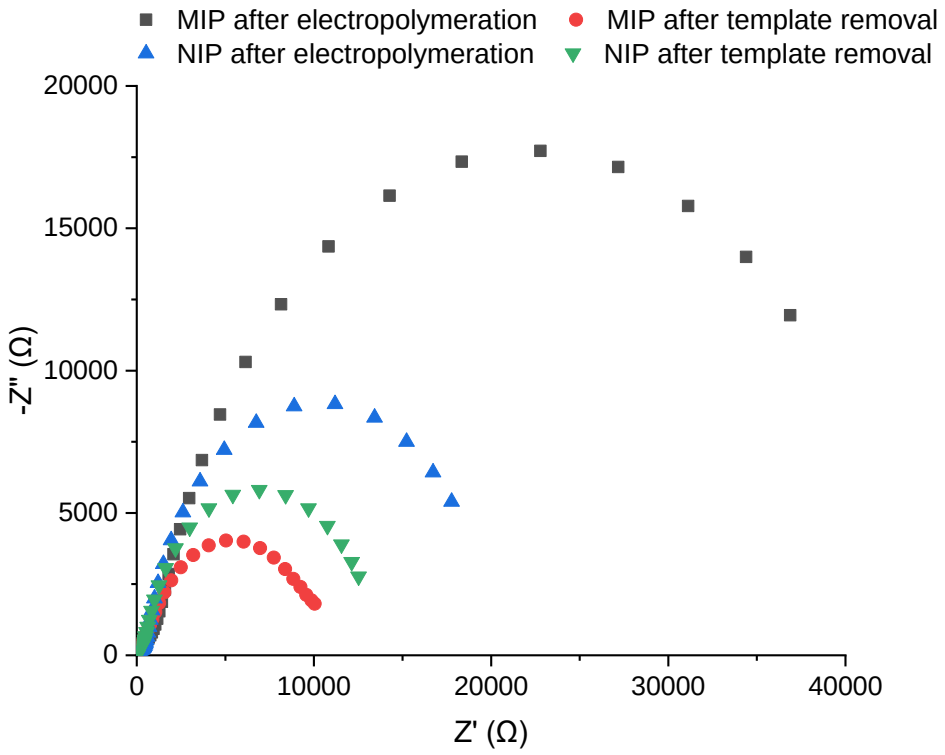

Figure 24 - Nyquist plots for MIP and NIP before and after template removal for 5 min.

Looking at Figure 24, it is noticeable that MIP presents a much higher Rct value after electropolymerization in comparison with the NIP one, which can be a strong indication of the presence of CRP entrapped inside the polymeric matrix, constituting a block to the electron charge transference. Afterwards, a higher removal percentage was observed on the MIP against the NIP which can prove the elution of the protein from the polymeric structure. Furthermore, the results after the removal step showed that the Rct values of NIP and MIP became very similar, meaning that the protein was successfully removed from the MIP structure.

4.1.3. Study of CRP concentration during the imprinting

Another important factor to be studied during the assembly of a MIP sensor is the concentration of template molecule used during the imprinting phase. It is important to emphasize that the protein concentration is fundamental for molecular imprinting, since the higher the concentration, the higher the number of protein imprints on the surface of the polymer matrix [99]. On the other hand, using a concentration too high may lead to saturation of the network [100].

Therefore, two different concentrations of CRP were tested during the electropolymerization step, 5 μg mL^{-1} and 0.5 μg mL^{-1}. Afterwards, the biosensor's performance was investigated by conducting the rebinding of CRP at different concentrations.

Figure 25 presents the Nyquist plots for MIP before and after template removal for CRP concentration of 5 μg mL^{-1} and 0.5 μg mL^{-1} and the respective calibration curves.

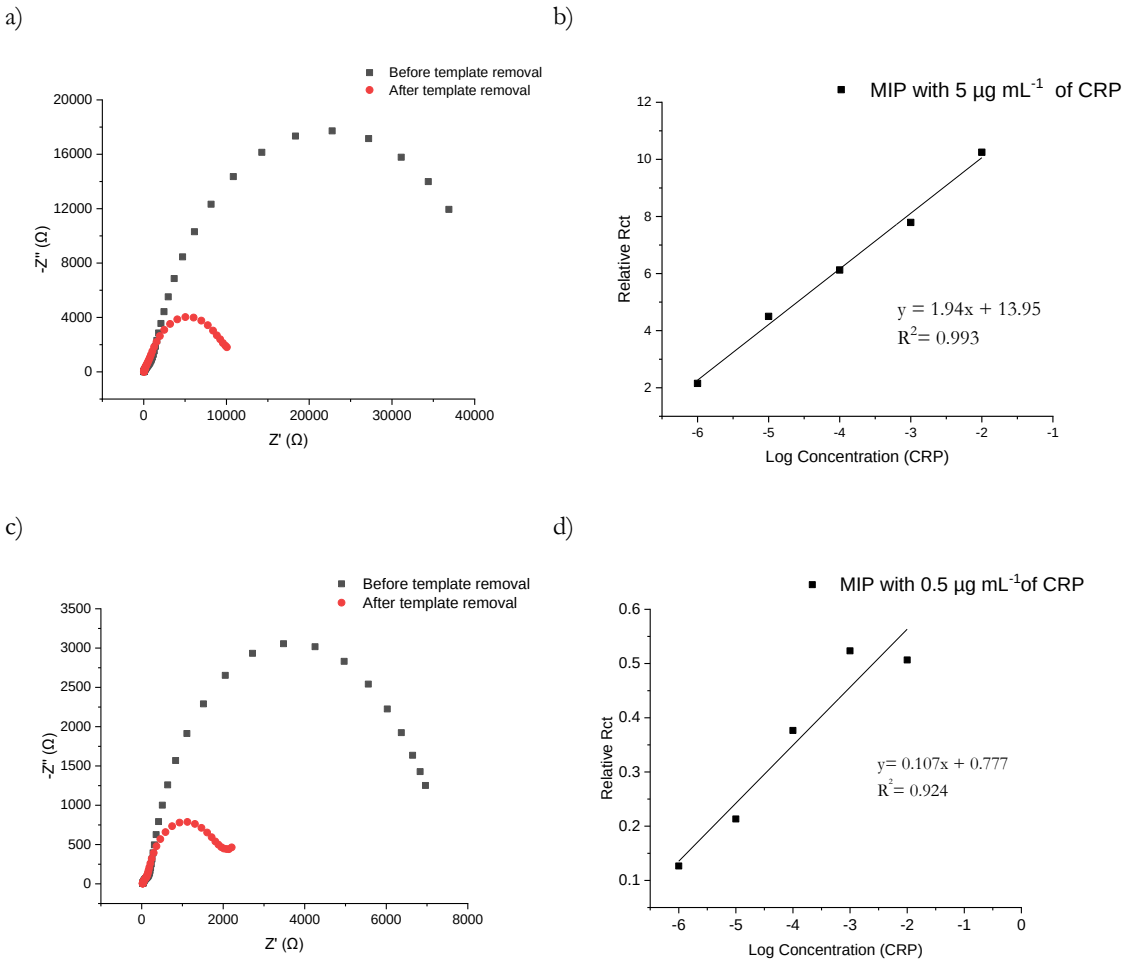

Figure 25 - a) Nyquist plots for MIP before and after template removal for CRP concentration 5 µg mL^{-1}; b) MIP calibration curve for CRP concentration 5 µg mL^{-1}; c) Nyquist plots for MIP before and after template removal for CRP concentration 0.5 µg mL^{-1}; d) MIP calibration curve for CRP concentration 0.5 µg mL^{-1}.

Inferring from the Nyquist plots that the presence of the protein serves as a barrier to the passage of passing electrons, it can be said that higher concentrations of CRP resulted in higher values of Rct (before template removal).

The MIP with 5 µg mL^{-1} of protein demonstrated greater sensitivity (slope of 1.94) and a higher R^2 (0.993) than the MIP with 0.5 µg mL^{-1} of protein (slope of 0.107 and R^2 of 0.924), according to the results obtained. These results were expected since the higher the concentration, the higher the number of impressions of it on the surface of the polymer matrix [99] .

Thus, it is reasonable to draw the conclusion that the MIP with 5 µg mL^{-1} of imprinted protein is the biosensor with the best outcomes, i.e., with the maximum linearity, reproducibility, and sensitivity.

4.2. Characterization study

4.2.1. FTIR analysis

Along the assembly process of the biosensor platform, each modification was verified by FTIR analysis. Thus, the following samples were analyzed: bare gold electrode cleaned with H_2SO_4 and MIP and NIP

sensors set up with 10 electropolymerization cycles. Thus, Figure 26 shows the graphs resulting from the FTIR analysis for different sensor materials.

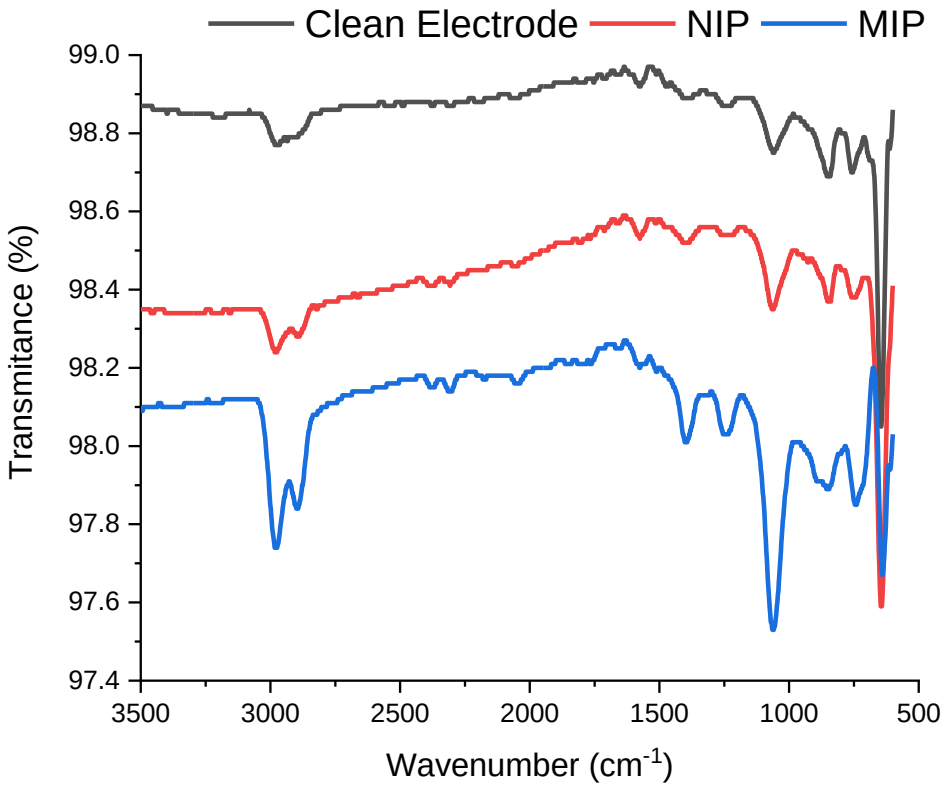

Figure 26 - FTIR analysis of the cleaned gold electrode, NIP and MIP electrodes.

As expected, both the MIP and NIP polymeric materials' FTIR spectra showed several comparable peaks, demonstrating their identical chemical compositions.

The functional groups contained in the polymer matrices were often disclosed by the largest peaks between the spectra. The formation of polymer was confirmed by the presence of some peals like at nearly 3000 cm^{-1} the aromatic C-H stretching, aromatic C=C stretching (benzene ring) at roughly 1600 and 1500 cm^{-1}, 1400 cm^{-1} of C-H deformation, 1250 cm^{-1} of C-N stretching, and 1000 cm^{-1} of C-O deformation were all observed [101], [102].

In addition, a band was found about 1500 cm^{-1}, which is predominantly present in MIP and can be ascribed to C-H stretching vibrations, demonstrating the existence of the protein, CRP, could be found in the FTIR spectra of MIP materials.

4.2.2. Raman analysis

During the last decade, Raman spectroscopy has matured into one of the most powerful techniques in analytical science due to its molecular sensitivity, its ease of application and the fact that, unlike infrared absorption spectroscopy, the presence of water does not impede its applicability [103].

Samples from each stage were examined: the bare electrode sample washed with H_2SO_4, the MIP stage and the NIP stage. Ten electropolymerization cycles were used for the MIP and NIP samples.

Thus, Figure 27 shows the graphs resulting from the Raman analysis for different sensor materials.

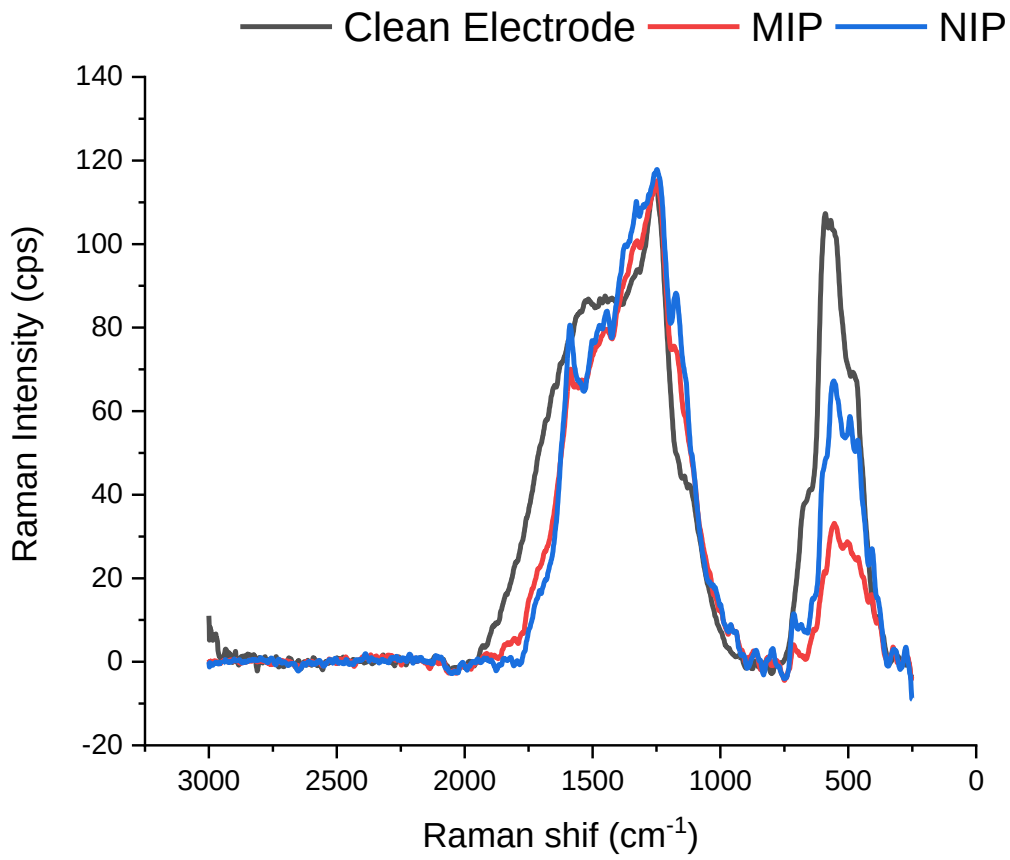

Figure 27- Resulting graphs of Raman analysis for different sensor materials.

The presence of peaks at ~1400 cm^{-1} was associated with the C-N stretching vibration, having an intermediate single/double bond order, and being associated with quinoid/benzene type rings present in the aniline constitution and therefore present in the MIP, NIP [101], [104]. In the region around 1650 cm^{-1}, the Raman peak spectrum was assigned to the carbon-carbon stretching vibrations of quinoid/benzene type rings [101].

The Raman spectra of the clean electrode showed 2 bands at 500, 550 cm^{-1} which can be attributed to carbon compounds present in the manufacture of the gold paint paste [105]. Comparison between the Au-SPE spectra and those modified with electropolymerization showed a substantial reduction in the intensity of the 550 cm^{-1} peak as a result of the polymer assembly, thus covering the gold surface [105].

By analyzing the Raman spectra, it is possible to confirm the surface modifications, since the intensity of the peaks decreases due to the formation of polymer. However, regarding the presence of CRP in the MIP, no major conclusions can be drawn since the MIP and NIP results are quite similar, probably due to the aromatic ring present in poly(aniline).

4.2.3. SEM analysis

All the different biosensor stages were morphologically characterized using SEM, one of the most popular ways to study the surface morphology. A low-energy electron beam is fired into the substance, then it travels across the sample's surface. Numerous interactions take place when the beam approaches and enters the material, leading to the emission of photons and electrons from or close to the sample's surface [106].

Each phase's samples were examined: the bare electrode sample washed with H_2SO_4, the sample polymerized with aniline alone, the MIP step, and the NIP step.

The different materials were analyzed to investigate the different modifications on the sensor surface. In this sense, Figure 28 shows the images obtained by SEM with an amplification of 1 000, 25 000, 50 000 and 100 000 X.

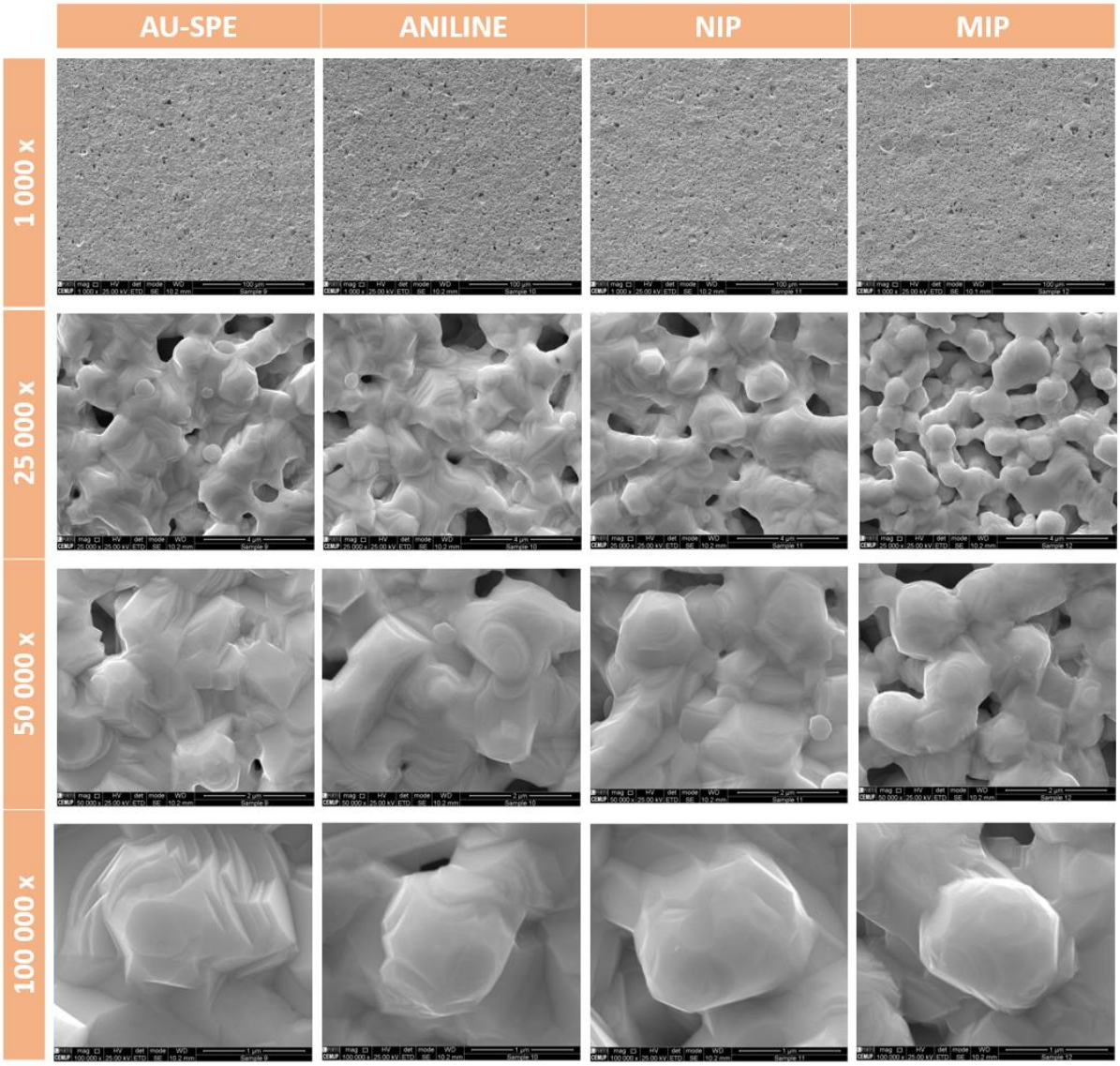

Figure 28 - SEM analysis results of different sensor materials at different magnifications (1 000, 25 000, 50 000 and 100 000 X).

According to the Figure 28, it is feasible to notice that following electropolymerization, a more homogeneous morphological layer is detected from the image of the bare gold electrodes.

Additionally, when comparing the electropolymerization with and without chitosan, it can be seen that the presence of chitosan (MIP and NIP) results in a more outlined look with less stringency, which demonstrates the avoidance of chitosan in the matrix.

An obvious morphological alteration is seen when comparing the differences between MIP and NIP. By looking to the MIP data (1 000 X amplification), it is easy to see that the surface is rougher with small islets that can be assigned to the presence of the entrapped protein.

4.3. Performance of the MIP sensor

4.3.1. Calibration Curve

The analytical performance of the CRP biosensing materials obtained by using aniline and chitosan mixture was assessed by recording calibration curves with the EIS technique after optimizing the most suitable experimental parameters regarding the electropolymerization process. First, the impact of a variable cycle count and scan rate was investigated. A thin, consistent, and homogeneous polymer covering must be created.

The procedure selected to the removal of the imprinted protein was a 4:1 dilution of methanol with acetic acid for 5 min, followed by a 30 min incubation in acetate buffer to stabilize the pH environment.

Then, seven consecutive concentrations of CRP were incubated during the sensor's development. However, it was discovered that the biosensor became saturated at 0.1 μg mL^{-1} of concentration. Since then, calibrations have only been carried out up to a concentration of 0.01 μg mL^{-1} (Figure 29).

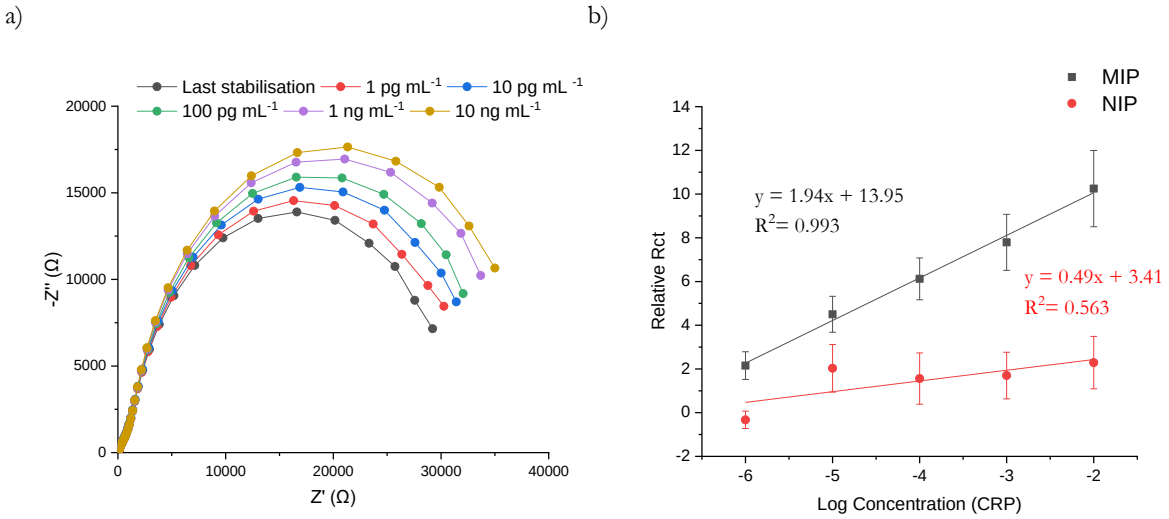

Figure 29 - a) EIS recordings for each standard concentration of a MIP; b) MIP and NIP calibration curve with error bars (triplicate experiments).

Thus, Figure 29 depicts the final MIP and NIP calibrations following the biosensor's assembly under optimal conditions. Because the protein target occupies the cavity locations in the MIP film, the Rct rises

as the concentration of CRP protein does, as expected. The error bars for each concentration constitute a strong indication of good reproducibility because they were carried out in triplicate. In contrast, the NIP control did not present a linear correlation. The limit of detection (LOD) was calculated using IUPAC protocol (LOD=3σ/slope) and it turned out to be 2.22 pg mL^{-1}, where σ concerns the standard deviation of blank measurements.

In order to evaluate the specificity performance of the assembled biosensors, the value of the imprinting factor (IF = [template rebound by MIP]/[template rebound by NIP]) can be also used as a comparative tool. From the ratio of sensitivity of the MIP sensor to CRP and to the NIP one, the IF was determined to be ~ 4.

4.3.2. Selectivity Study

One important requirement in the development and optimization of a biosensing platform is its ability to recognize and quantify a specific target molecule in a complex mixture containing other compounds (or interferents). Herein, the main purpose of this biosensor is to be used for inflammation assessment for chronic wound application. Like mentioned before, chronic wounds are commonly defined as wounds that have not reduced in size by more than 40% to 50% or healed within one month. The global prevalence of chronic wounds is estimated at 1.51 to 2.21 per 1000 population, and the incidence is expected to rise with ageing populations worldwide [107]. Some of the elements in chronic wound fluid are shown in Table 6.

Table 6 - Some constituents of chronic wound fluid.

Constituent	Description	Reference
CRP	Infection and inflammation markers are produced in response to the presence of invasive agents.	[108], [109]
IgG, IgA, IgM, IgD, IgE	Antibody that represents the body's defense against bacteria found in the wound.	[109]
IL-6, IL-1, TNF-α, TNF-β	Cytokine that promotes healing and controls the inflammatory response.	[109]
Glucose	Simple sugar that may be present in wounds with infection.	[108], [109]
Proteolytic Enzymes	Examples include Matrix Metalloproteinases (MMPs), which are involved in the breakdown of the extracellular matrix.	[108]
Fibrin	Protein that is involved in the temporary clot development to cover the wound.	[108]
Inflammatory Cells	Leukocytes, such as neutrophils and macrophages, which are engaged in tissue defense and repair, are one example.	[108]
Creatinine, Urea	Utilized as indicators of renal health in clinical settings to evaluate kidney function	[109]

Subsequently, the selectivity of the biosensor was investigated in order to understand its ability to distinguish CRP in a medium with potential interferents.

Thus, three of the most important elements present in these wound fluids were chosen from the components displayed. IL-6 is a critical marker of infection and inflammation in the wound. Additionally, the presence of IgG represents the immune system's reaction to the presence of germs, whereas glucose is a crucial substance that might affect the wound's metabolic balance. Therefore, to verify the selectivity of the sensory device, IL-6, IgG and glucose were herein selected as interfering species.

Figure 30 shows the EIS data regarding the three interferents incubated in the MIP sensors.

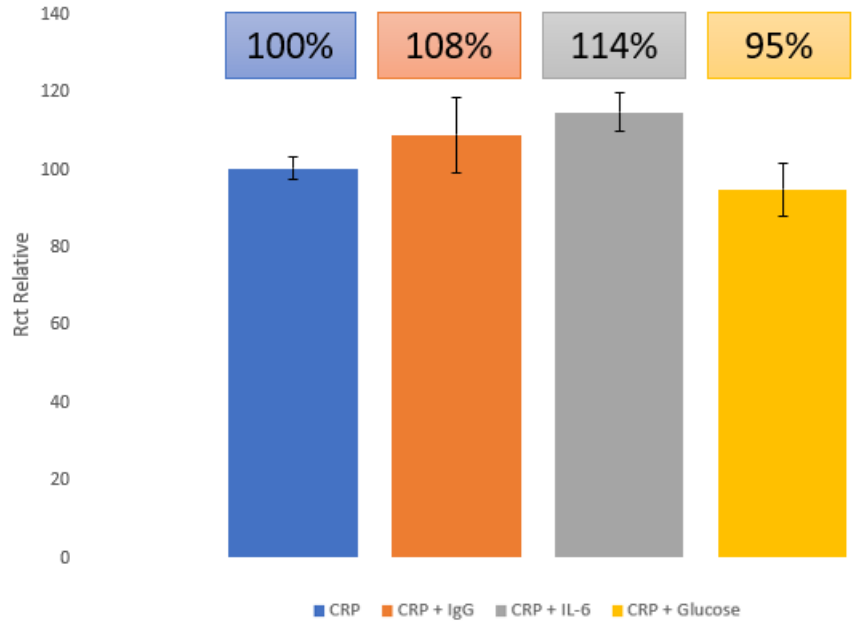

Figure 30 - Graph representing the results of the selectivity test performed for different interfering species.

All the tested molecules presented less than 15% of interference and, with a 14% difference from the CRP signal, IL-6 was the interferent with the largest influence on the biosensor response, according to the study of Figure 30.

There was no statistically significant difference between the groups, according to a one-way Anova test (P=0.05) that was also carried out.

Overall, these findings give a strong indication that the biosensor can deliver a specific response for CRP detection.

5. CONCLUSION

In this chapter, the final conclusions of the work as well as its considerations and future research are presented.

5.1. Final conclusions

An adaptive reaction known as inflammation is typically brought on by unpleasant stimuli and diseases such widespread infection and/or tissue damage. The incidence of chronic wounds is predicted to rise as the world's population ages, with an estimated 1.51 to 2.21 per 1000 people globally.

Currently, new, quick, and simple methods for tracking inflammation still need to be developed. In this work, electrochemical biosensors—which have recently attracted special attention in the widest range of application fields—are put up as an alternative to more traditional and evasive detection techniques. Several drawbacks of more traditional approaches, including sensitivity, repeatability, detection limit, and stability, have been solved through its development.

The major goal of this research was to create an electrochemical biosensor for monitoring chronic wounds that had strong stability and repeatability features. The target molecule was specifically chosen to be CRP, an inflammatory biomarker. The recognition component was created using molecular imprinting technology, which over natural antibodies offers several benefits in terms of chemical stability, general manufacturing simplicity, and cheap production costs.

In order to create a polymeric matrix with functional groups that would increase the affinity between the polymer and the protein, various optimizations were carried out in the experimental development of this dissertation, including electrode functionalization (number of scan-rates and cycles) and type of monomers for electropolymerization were investigated.

It is important to pick the right monomer since its functional groups will engage with certain protein locations and enable a more customized molecular imprinting process. Thus, to build the MIP in Au-SPE platform, aniline was used as the electropolymerizable monomer. The addition of chitosan enhances the biosensor's stability and toughness for the detection of target analytes, suggesting improvements in environmental and health monitoring.

The optimal electropolymerization conditions accomplished were a potential range of [-0.6; +1.0] V, for 5 cycles at 0.05 Vs^{-1} scan rate. The ideal CRP concentration for imprinting was also researched. The optimized response was obtained with a CRP concentration of 5 $\mu g\ mL^{-1}$, demonstrating good sensitivity and linearity. An acid-organic mixture that shouldn't significantly alter or degrade the NIP material was used to maximize the removal of CRP from the polymeric matrix. Methanol and acetic acid were used to conduct the removal, and then the WE surface was incubated in a buffer to regulate the pH.

In addition, methods including SEM, Raman spectroscopy, and FTIR were used to analyze the biosensor's surface.

These methods were utilized to keep track of and validate the changes made at each stage of the biosensor manufacturing process. All methods revealed minute variations between the NIP and MIP sensors, which is proof that the protein was present throughout MIP development.

It was feasible to demonstrate the effectiveness of the various alterations made to the surface of the sensor material with the help of these additional chemical methods and analyses of material structure.

Overall, the MIP-based sensor demonstrated strong electrochemical response, good repeatability, quick reaction time (30 min of incubation), selectivity, and stability in the CRP concentration range of 0.001 ng μg mL^{-1} to 0.01 μg mL^{-1}. The LOD obtained in this work shows lower values when compared to other sensors in the same area (Table 1).

This innovative method opens the door to reliable, timely, and least invasive identification of biomarkers linked to inflammation.

5.2. Future perspetives

Future research should focus on the incorporation of the developed sensing construction into a flexible platform that is suitable for wearable application and biocompatible to come into contact with human skin.

Furthermore, as the optimal CRP concentration range in biological samples is in the range of milligrams, the detection concentration range of the biosensor can be tuned in order to be used as an in-situ tool for assessment of inflammation events.

REFERENCES

[1] R. Medzhitov, "Origin and physiological roles of inflammation," *Nature 2008 454:7203*, vol. 454, no. 7203, pp. 428–435, Jul. 2008, doi: 10.1038/nature07201.

[2] "Inflammation: What Is It, Causes, Symptoms & Treatment." https://my.clevelandclinic.org/health/symptoms/21660-inflammation (accessed Mar. 30, 2023).

[3] J. M. Bennett, G. Reeves, G. E. Billman, and J. P. Sturmberg, "Inflammation-nature's way to efficiently respond to all types of challenges: Implications for understanding and managing 'the epidemic' of chronic diseases," *Front Med (Lausanne)*, vol. 5, no. NOV, 2018, doi: 10.3389/FMED.2018.00316/FULL.

[4] S. Hannoodee and D. N. Nasuruddin, "Acute Inflammatory Response," *Nature*, vol. 206, no. 4979, p. 20, Nov. 2022, doi: 10.1038/206020a0.

[5] H. B. Fleit, "Chronic Inflammation," *Pathobiology of Human Disease: A Dynamic Encyclopedia of Disease Mechanisms*, pp. 300–314, Jan. 2014, doi: 10.1016/B978-0-12-386456-7.01808-6.

[6] R. Pahwa, A. Goyal, and I. Jialal, "Chronic Inflammation," *Pathobiology of Human Disease: A Dynamic Encyclopedia of Disease Mechanisms*, pp. 300–314, Aug. 2022, doi: 10.1016/B978-0-12-386456-7.01808-6.

[7] "What is Chronic Inflammation (and How to Treat It)." https://www.healthline.com/health/chronic-inflammation#symptoms (accessed Mar. 30, 2023).

[8] N. R. Sproston and J. J. Ashworth, "Role of C-reactive protein at sites of inflammation and infection," *Front Immunol*, vol. 9, no. APR, p. 754, Apr. 2018, doi: 10.3389/FIMMU.2018.00754/BIBTEX.

[9] A. Mobasheri, "Biosensors for the Multiplex Detection of Inflammatory Disease Biomarkers," *Biosensors 2021, Vol. 11, Page 11*, vol. 11, no. 1, p. 11, Dec. 2020, doi: 10.3390/BIOS11010011.

[10] "BioMark Sensor Research." https://www.biomark.isep.ipp.pt/pt/home/ (accessed Mar. 30, 2023).

[11] "A current view on inflammation," *Nature Immunology 2017 18:8*, vol. 18, no. 8, pp. 825–825, Jul. 2017, doi: 10.1038/ni.3798.

[12] L. Chen *et al.*, "Inflammatory responses and inflammation-associated diseases in organs," *Oncotarget*, vol. 9, no. 6, p. 7204, Jan. 2018, doi: 10.18632/ONCOTARGET.23208.

[13] M. S. Ellulu and H. Samouda, "Clinical and biological risk factors associated with inflammation in patients with type 2 diabetes mellitus," *BMC Endocr Disord*, vol. 22, no. 1, pp. 1–10, Dec. 2022, doi: 10.1186/S12902-021-00925-0/FIGURES/2.

[14] G. G. Mackenzie, "Inflammation and cancer," *Cancer Immunology and Immunotherapy: Volume 1 of Delivery Strategies and Engineering Technologies in Cancer Immunotherapy*, pp. 63–82, Jan. 2022, doi: 10.1016/B978-0-12-823397-9.00003-X.

[15] L. Ferrucci and E. Fabbri, "Inflammageing: chronic inflammation in ageing, cardiovascular disease, and frailty," *Nature Reviews Cardiology 2018 15:9*, vol. 15, no. 9, pp. 505–522, Jul. 2018, doi: 10.1038/s41569-018-0064-2.

[16] J. Kusumah and E. Gonzalez de Mejia, "Impact of soybean bioactive compounds as response to diet-induced chronic inflammation: A systematic review," *Food Research International*, vol. 162, p. 111928, Dec. 2022, doi: 10.1016/J.FOODRES.2022.111928.

[17] J. Kusumah and E. Gonzalez de Mejia, "Impact of soybean bioactive compounds as response to diet-induced chronic inflammation: A systematic review," *Food Research International*, vol. 162, p. 111928, Dec. 2022, doi: 10.1016/J.FOODRES.2022.111928.

[18] "Inflammatory markers explained - ARC West." https://arc-w.nihr.ac.uk/news/inflammatory-markers-explained/ (accessed Mar. 30, 2023).

[19] "C-Reactive Protein (CRP) Test: MedlinePlus Medical Test." https://medlineplus.gov/lab-tests/c-reactive-protein-crp-test/ (accessed Mar. 30, 2023).

[20] "Should you be tested for inflammation? - Harvard Health." https://www.health.harvard.edu/blog/should-you-be-tested-for-inflammation-202203292715 (accessed Mar. 30, 2023).

[21] "Plasma viscosity." https://labtestsonline.org.uk/tests/plasma-viscosity (accessed Mar. 30, 2023).

[22] A. Kotulska, M. Kopeć-Mędrek, A. Grosicka, M. Kubicka, and E. J. Kucharz, "Correlation between erythrocyte sedimentation rate and C-reactive protein level in patients with rheumatic diseases," *Reumatologia*, vol. 53, no. 5, pp. 243–246, 2015, doi: 10.5114/REUM.2015.55825.

[23] S. K. Vashist, A. G. Venkatesh, E. Marion Schneider, C. Beaudoin, P. B. Luppa, and J. H. T. Luong, "Bioanalytical advances in assays for C-reactive protein," *Biotechnol Adv*, vol. 34, no. 3, pp. 272–290, May 2016, doi: 10.1016/J.BIOTECHADV.2015.12.010.

[24] Y. Y. Luan and Y. M. Yao, "The clinical significance and potential role of C-reactive protein in chronic inflammatory and neurodegenerative diseases," *Front Immunol*, vol. 9, no. JUN, p. 1302, Jun. 2018, doi: 10.3389/FIMMU.2018.01302/BIBTEX.

[25] A. Pfützner, T. Schöndorf, M. Hanefeld, and T. Forst, "High-Sensitivity C-Reactive Protein Predicts Cardiovascular Risk in Diabetic and Nondiabetic Patients: Effects of Insulin-Sensitizing Treatment with Pioglitazone," *https://doi.org/10.1177/193229681000400326*, vol. 4, no. 3, pp. 706–716, May 2010, doi: 10.1177/193229681000400326.

[26] S. Balayan, N. Chauhan, W. Rosario, and U. Jain, "Biosensor development for C-reactive protein detection: A review," *Applied Surface Science Advances*, vol. 12, p. 100343, Dec. 2022, doi: 10.1016/J.APSADV.2022.100343.

[27] S. Black, I. Kushner, and D. Samols, "C-reactive protein," *Journal of Biological Chemistry*, vol. 279, no. 47, pp. 48487–48490, Nov. 2004, doi: 10.1074/jbc.R400025200.

[28] A. Koyun, E. Ahlatcıoğlu, Y. K. İpek, A. Koyun, E. Ahlatcıoğlu, and Y. K. İpek, "Biosensors and Their Principles," *A Roadmap of Biomedical Engineers and Milestones*, Jun. 2012, doi: 10.5772/48824.

[29] D. R. Thévenot, K. Toth, R. A. Durst, and G. S. Wilson, "Electrochemical biosensors: recommended definitions and classification," *Biosens Bioelectron*, vol. 16, no. 1–2, pp. 121–131, Jan. 2001, doi: 10.1016/S0956-5663(01)00115-4.

[30] N. Bhalla, P. Jolly, N. Formisano, and P. Estrela, "Introduction to biosensors," *Essays Biochem*, vol. 60, no. 1, p. 1, Jun. 2016, doi: 10.1042/EBC20150001.

[31] "View of An insight into the multifarious applications of biosensors and the way forward." http://jddtonline.info/index.php/jddt/article/view/5633/5010 (accessed Mar. 30, 2023).

[32] S. P. Mohanty and E. Koucianos, "Biosensors: A tutorial review," *IEEE Potentials*, vol. 25, no. 2, pp. 35–40, 2006, doi: 10.1109/MP.2006.1649009.

[33] A. Herrera-Chacón, X. Cetó, and M. del Valle, "Molecularly imprinted polymers - towards electrochemical sensors and electronic tongues," *Anal Bioanal Chem*, vol. 413, no. 24, pp. 6117–6140, Oct. 2021, doi: 10.1007/S00216-021-03313-8/METRICS.

[34] J. J. Belbruno, "Molecularly Imprinted Polymers," *Chem Rev*, vol. 119, no. 1, pp. 94–119, Jan. 2019, doi: 10.1021/ACS.CHEMREV.8B00171/ASSET/IMAGES/LARGE/CR-2018-00171R_0010.JPEG.

[35] F. Yemiş, "Molecularly Imprinted Polymers and Their Synthesis by Different Methods," *Polymers & Polymer Composites*, vol. 21, no. 3, 2013.

[36] Z. El-Schich *et al.*, "Molecularly imprinted polymers in biological applications," *Biotechniques*, vol. 69, no. 6, pp. 407–420, Dec. 2020, doi: 10.2144/BTN-2020-0091/ASSET/IMAGES/LARGE/FIGURE6.JPEG.

[37] S. Asliyuce, L. Uzun, A. Yousefi Rad, S. Unal, R. Say, and A. Denizli, “Molecular imprinting based composite cryogel membranes for purification of anti-hepatitis B surface antibody by fast protein liquid chromatography,” *Journal of Chromatography B*, vol. 889–890, pp. 95–102, Mar. 2012, doi: 10.1016/J.JCHROMB.2012.02.001.

[38] H. Zhang, L. Ye, and K. Mosbach, “Non-covalent molecular imprinting with emphasis on its application in separation and drug development,” *Journal of Molecular Recognition*, vol. 19, no. 4, pp. 248–259, Jul. 2006, doi: 10.1002/JMR.793.

[39] M. Kempe and K. Mosbach, “Molecular imprinting used for chiral separations,” *J Chromatogr A*, vol. 694, no. 1, pp. 3–13, Mar. 1995, doi: 10.1016/0021-9673(94)01070-U.

[40] S. Vidyasankar and F. H. Arnold, “Molecular imprinting: selective materials for separations, sensors and catalysis,” *Curr Opin Biotechnol*, vol. 6, no. 2, pp. 218–224, Jan. 1995, doi: 10.1016/0958-1669(95)80036-0.

[41] G. Ertürk, L. Uzun, M. A. Tümer, R. Say, and A. Denizli, “Fab fragments imprinted SPR biosensor for real-time human immunoglobulin G detection,” *Biosens Bioelectron*, vol. 28, no. 1, pp. 97–104, Oct. 2011, doi: 10.1016/J.BIOS.2011.07.004.

[42] P. A. G. Cormack and A. Z. Elorza, “Molecularly imprinted polymers: synthesis and characterisation,” *Journal of Chromatography B*, vol. 804, no. 1, pp. 173–182, May 2004, doi: 10.1016/J.JCHROMB.2004.02.013.

[43] G. Ertürk and B. Mattiasson, “Molecular Imprinting Techniques Used for the Preparation of Biosensors,” *Sensors 2017, Vol. 17, Page 288*, vol. 17, no. 2, p. 288, Feb. 2017, doi: 10.3390/S17020288.

[44] A. Herrera-Chacón, X. Cetó, and M. del Valle, “Molecularly imprinted polymers - towards electrochemical sensors and electronic tongues,” *Anal Bioanal Chem*, vol. 413, no. 24, pp. 6117–6140, Oct. 2021, doi: 10.1007/S00216-021-03313-8/METRICS.

[45] G. Ertürk and B. Mattiasson, “Molecular Imprinting Techniques Used for the Preparation of Biosensors,” *Sensors (Basel)*, vol. 17, no. 2, Feb. 2017, doi: 10.3390/S17020288.

[46] V. Naresh and N. Lee, “A review on biosensors and recent development of nanostructured materials-enabled biosensors,” *Sensors (Switzerland)*, vol. 21, no. 4. MDPI AG, pp. 1–35, Feb. 02, 2021. doi: 10.3390/s21041109.

[47] M. F. Frasco, L. A. A. N. A. Truta, M. G. F. Sales, and F. T. C. Moreira, “Imprinting technology in electrochemical biomimetic sensors,” *Sensors (Switzerland)*, vol. 17, no. 3. MDPI AG, Mar. 06, 2017. doi: 10.3390/s17030523.

[48] D. R. Thévenot, K. Toth, R. A. Durst, and G. S. Wilson, “Electrochemical biosensors: recommended definitions and classification,” *Biosens Bioelectron*, vol. 16, no. 1–2, pp. 121–131, Jan. 2001, doi: 10.1016/S0956-5663(01)00115-4.

[49] V. Suryanarayanan, C. T. Wu, and K. C. Ho, “Molecularly imprinted electrochemical sensors,” *Electroanalysis*, vol. 22, no. 16, pp. 1795–1811, Aug. 2010, doi: 10.1002/ELAN.200900616.

[50] J. Baranwal, B. Barse, G. Gatto, G. Broncova, and A. Kumar, “Electrochemical Sensors and Their Applications: A Review,” *Chemosensors*, vol. 10, no. 9. MDPI, Sep. 01, 2022. doi: 10.3390/chemosensors10090363.

[51] O. Gharbi, M. T. T. Tran, B. Tribollet, M. Turmine, and V. Vivier, “Revisiting cyclic voltammetry and electrochemical impedance spectroscopy analysis for capacitance measurements,” *Electrochim Acta*, vol. 343, p. 136109, May 2020, doi: 10.1016/J.ELECTACTA.2020.136109.

[52] N. N. Elgrishi, K. J. Rountree, B. D. Mccarthy, E. S. Rountree, T. T. Eisenhart, and J. L. Dempsey, “A Practical Beginner’s Guide to Cyclic Voltammetry,” 2017, doi: 10.1021/acs.jchemed.7b00361.

[53] I. J. Cutress, E. J. F. Dickinson, and R. G. Compton, “Analysis of commercial general engineering finite element software in electrochemical simulations,” *Journal of Electroanalytical Chemistry*, vol. 638, no. 1, pp. 76–83, Jan. 2010, doi: 10.1016/J.JELECHEM.2009.10.017.

[54] W. F. Pacheco, F. S. Semaan, V. G. K. De Almeida, A. G. S. L. Ritta, and R. Q. Aucélio, "Voltametrias: Uma Breve Revisão Sobre os Conceitos," *Revista Virtual de Química*, vol. 5, no. 4, pp. 516–537, Aug. 2013, doi: 10.5935/1984-6835.20130040.

[55] "Voltammetric and Amperometric Sensors".

[56] H. S. Magar, R. Y. A. Hassan, and A. Mulchandani, "Electrochemical Impedance Spectroscopy (EIS): Principles, Construction, and Biosensing Applications," *Sensors (Basel)*, vol. 21, no. 19, Oct. 2021, doi: 10.3390/S21196578.

[57] S. Wang, J. Zhang, O. Gharbi, V. Vivier, M. Gao, and M. E. Orazem, "Electrochemical impedance spectroscopy," *Nature Reviews Methods Primers 2021 1:1*, vol. 1, no. 1, pp. 1–21, Jun. 2021, doi: 10.1038/s43586-021-00039-w.

[58] B.-A. Mei, O. Munteshari, J. Lau, B. Dunn, and L. Pilon, "Physical Interpretations of Nyquist Plots for EDLC Electrodes and Devices," *J. Phys. Chem. C*, vol. 122, p. 2023, 2018, doi: 10.1021/acs.jpcc.7b10582.

[59] "Gráfico de Nyquist para Medição de Impedância de Baterias de Íons de Lítio | Hioki." https://www.hioki.com/br-pt/learning/electricity/nyquist.html (accessed Mar. 30, 2023).

[60] Z. Taleat, A. Khoshroo, and M. Mazloum-Ardakani, "Screen-printed electrodes for biosensing: A review (2008-2013)," *Microchimica Acta*, vol. 181, no. 9–10, pp. 865–891, Apr. 2014, doi: 10.1007/S00604-014-1181-1/FIGURES/3.

[61] D. M. Heard and A. J. J. Lennox, "Electrode Materials in Modern Organic Electrochemistry," *Angewandte Chemie - International Edition*, vol. 59, no. 43, pp. 18866–18884, Oct. 2020, doi: 10.1002/ANIE.202005745.

[62] M. D. Kärkäs, "Electrochemical strategies for C–H functionalization and C–N bond formation," *Chem Soc Rev*, vol. 47, no. 15, pp. 5786–5865, Jul. 2018, doi: 10.1039/C7CS00619E.

[63] M. P. Nair, A. J. T. Teo, and K. H. H. Li, "Acoustic biosensors and microfluidic devices in the decennium: Principles and applications," *Micromachines (Basel)*, vol. 13, no. 1, p. 24, Jan. 2022, doi: 10.3390/MI13010024/S1.

[64] L. O. Resende, A. C. H. de Castro, A. O. Andrade, J. M. Madurro, and A. G. Brito-Madurro, "Immunosensor for electrodetection of the C-reactive protein in serum," *Journal of Solid State Electrochemistry*, vol. 22, no. 5, pp. 1365–1372, May 2018, doi: 10.1007/S10008-017-3820-Z/FIGURES/6.

[65] T. Bryan, X. Luo, P. R. Bueno, and J. J. Davis, "An optimised electrochemical biosensor for the label-free detection of C-reactive protein in blood," *Biosens Bioelectron*, vol. 39, no. 1, pp. 94–98, Jan. 2013, doi: 10.1016/J.BIOS.2012.06.051.

[66] M. Jarczewska, J. Rębiś, Ł. Górski, and E. Malinowska, "Development of DNA aptamer-based sensor for electrochemical detection of C-reactive protein," *Talanta*, vol. 189, pp. 45–54, Nov. 2018, doi: 10.1016/J.TALANTA.2018.06.035.

[67] D. Kumar and B. B. Prasad, "Multiwalled carbon nanotubes embedded molecularly imprinted polymer-modified screen printed carbon electrode for the quantitative analysis of C-reactive protein," *Sens Actuators B Chem*, vol. 171–172, pp. 1141–1150, Aug. 2012, doi: 10.1016/J.SNB.2012.06.053.

[68] M. Cui, Z. Che, Y. Gong, T. Li, W. Hu, and S. Wang, "A graphdiyne-based protein molecularly imprinted biosensor for highly sensitive human C-reactive protein detection in human serum," *Chemical Engineering Journal*, vol. 431, p. 133455, Mar. 2022, doi: 10.1016/J.CEJ.2021.133455.

[69] R. K. Gupta, A. Periyakaruppan, M. Meyyappan, and J. E. Koehne, "Label-free detection of C-reactive protein using a carbon nanofiber based biosensor," *Biosens Bioelectron*, vol. 59, pp. 112–119, Sep. 2014, doi: 10.1016/J.BIOS.2014.03.027.

[70] I. Macwan, A. Aphale, P. Bhagvath, S. Prasad, and P. Patra, "Detection of Cardiovascular CRP Protein Biomarker Using a Novel Nanofibrous Substrate", doi: 10.3390/bios10060072.

[71] Á. Molinero-Fernández, L. Arruza, M. Á. López, and A. Escarpa, "On-the-fly rapid immunoassay for neonatal sepsis diagnosis: C-reactive protein accurate determination using

magnetic graphene-based micromotors," *Biosens Bioelectron*, vol. 158, p. 112156, Jun. 2020, doi: 10.1016/J.BIOS.2020.112156.

[72] gueda Molinero-Ferna, ngel Lo, and A. Escarpa, "Electrochemical Microfluidic Micromotors-Based Immunoassay for C-Reactive Protein Determination in Preterm Neonatal Samples with Sepsis Suspicion," 2020, doi: 10.1021/acs.analchem.9b05384.

[73] A. K. Yagati, J. C. Pyun, J. Min, and S. Cho, "Label-free and direct detection of C-reactive protein using reduced graphene oxide-nanoparticle hybrid impedimetric sensor," *Bioelectrochemistry*, vol. 107, pp. 37–44, Feb. 2016, doi: 10.1016/J.BIOELECHEM.2015.10.002.

[74] T. Goda, M. Toya, A. Matsumoto, and Y. Miyahara, "Poly(3,4-ethylenedioxythiophene) Bearing Phosphorylcholine Groups for Metal-Free, Antibody-Free, and Low-Impedance Biosensors Specific for C-Reactive Protein," 2015, doi: 10.1021/acsami.5b09325.

[75] M. Jarczewska, R. Ziółkowski, Ł. Górski, and E. Malinowska, "Application of RNA Aptamers as Recognition Layers for the Electrochemical Analysis of C-Reactive Protein," *Electroanalysis*, vol. 30, no. 4, pp. 658–664, Apr. 2018, doi: 10.1002/ELAN.201700620.

[76] S. Balayan, N. Chauhan, R. Chandra, and U. Jain, "Electrochemical based c-reactive protein (Crp) sensing through molecularly imprinted polymer (mip) pore structure coupled with bi-metallic tuned screen-printed electrode," *Biointerface Res Appl Chem*, vol. 12, no. 6, pp. 7697–7714, Dec. 2022, doi: 10.33263/BRIAC126.76977714.

[77] S. Balayan, N. Chauhan, R. Chandra, and U. Jain, "Molecular imprinting based electrochemical biosensor for identification of serum amyloid A (SAA), a neonatal sepsis biomarker," *Int J Biol Macromol*, vol. 195, pp. 589–597, Jan. 2022, doi: 10.1016/J.IJBIOMAC.2021.12.045.

[78] E. Mazzotta, T. Di Giulio, and C. Malitesta, "Electrochemical sensing of macromolecules based on molecularly imprinted polymers: challenges, successful strategies, and opportunities," *Analytical and Bioanalytical Chemistry*, vol. 414, no. 18. Springer Science and Business Media Deutschland GmbH, pp. 5165–5200, Jul. 01, 2022. doi: 10.1007/s00216-022-03981-0.

[79] C. P. Jiménez-Gómez and J. A. Cecilia, "Chitosan: A Natural Biopolymer with a Wide and Varied Range of Applications," *Molecules*, vol. 25, no. 17. MDPI AG, Sep. 01, 2020. doi: 10.3390/molecules25173981.

[80] R. Petrucci, M. Pasquali, F. A. Scaramuzzo, and A. Curulli, "Recent advances in electrochemical chitosan-based chemosensors and biosensors: Applications in food safety," *Chemosensors*, vol. 9, no. 9. MDPI, Sep. 01, 2021. doi: 10.3390/chemosensors9090254.

[81] M. Beygisangchin, S. Abdul Rashid, S. Shafie, A. R. Sadrolhosseini, and H. N. Lim, "Preparations, Properties, and Applications of Polyaniline and Polyaniline Thin Films—A Review," *Polymers (Basel)*, vol. 13, no. 12, p. 2003, Jun. 2021, doi: 10.3390/polym13122003.

[82] S. El Aggadi, N. Loudiyi, A. Chadil, Z. El Abbassi, and A. El Hourch, "Electropolymerization of aniline monomer and effects of synthesis conditions on the characteristics of synthesized polyaniline thin films," *Mediterranean Journal of Chemistry*, vol. 10, no. 2, pp. 138–145, Feb. 2020, doi: 10.13171/mjc102020021114sea.

[83] S. Kobayashi, H. Uyama, and S. Kimura, "Enzymatic Polymerization," *Chem Rev*, vol. 101, no. 12, pp. 3793–3818, Dec. 2001, doi: 10.1021/cr990121l.

[84] R. A. de Barros, W. M. de Azevedo, and F. M. de Aguiar, "Photo-induced polymerization of polyaniline," *Mater Charact*, vol. 50, no. 2–3, pp. 131–134, Mar. 2003, doi: 10.1016/S1044-5803(03)00080-9.

[85] S. El Aggadi, N. Loudiyi, A. Chadil, Z. El Abbassi, and A. El Hourch, "Electropolymerization of aniline monomer and effects of synthesis conditions on the characteristics of synthesized polyaniline thin films," *Mediterranean Journal of Chemistry*, vol. 10, no. 2, pp. 138–145, Feb. 2020, doi: 10.13171/mjc102020021114sea.

[86] M. Beygisangchin, S. A. Rashid, S. Shafie, A. R. Sadrolhosseini, and H. N. Lim, “Preparations, properties, and applications of polyaniline and polyaniline thin films—a review,” *Polymers (Basel)*, vol. 13, no. 12, Jun. 2021, doi: 10.3390/polym13122003.

[87] A. D. Jannakoudakis, P. D. Jannakoudakis, N. Pagalos, and E. Theodoridou, “Electro-oxidation of aniline and electrochemical behaviour of the produced polyaniline film on carbon-fibre electrodes in aqueous methanolic solutions,” *Electrochim Acta*, vol. 38, no. 11, pp. 1559–1566, Aug. 1993, doi: 10.1016/0013-4686(93)80290-G.

[88] “FISPQ-Anilina”.

[89] “Spray drying parameters optimization for chitosan microparticles as insulin carrier,” 2003. [Online]. Available: https://www.researchgate.net/publication/289188339

[90] A. G. Yavuz, A. Uygun, and V. R. Bhethanabotla, “Preparation of substituted polyaniline/chitosan composites by in situ electropolymerization and their application to glucose sensing,” *Carbohydr Polym*, vol. 81, no. 3, pp. 712–719, Jul. 2010, doi: 10.1016/j.carbpol.2010.03.045.

[91] S. M. Bashir *et al.*, “Chitosan Nanoparticles: A Versatile Platform for Biomedical Applications,” *Materials*, vol. 15, no. 19. MDPI, Oct. 01, 2022. doi: 10.3390/ma15196521.

[92] A. Vacca, M. Mascia, S. Rizzardini, S. Palmas, and L. Mais, “Coating of gold substrates with polyaniline through electrografting of aryl diazonium salts,” *Electrochim Acta*, vol. 126, pp. 81–89, Apr. 2014, doi: 10.1016/j.electacta.2013.08.187.

[93] L. A. Potempa, Z.-Y. Yao, S.-R. Ji, J. G. Filep, and Y. Wu, “Solubilization and purification of recombinant modified C-reactive protein from inclusion bodies using reversible anhydride modification,” *Biophys Rep*, vol. 1, no. 1, pp. 18–33, Aug. 2015, doi: 10.1007/s41048-015-0003-2.

[94] G. Ziyatdinova, E. Guss, and E. Yakupova, “Electrochemical sensors based on the electropolymerized natural phenolic antioxidants and their analytical application,” *Sensors*, vol. 21, no. 24. MDPI, Dec. 01, 2021. doi: 10.3390/s21248385.

[95] S. Goswami, S. Nandy, E. Fortunato, and R. Martins, “Polyaniline and its composites engineering: A class of multifunctional smart energy materials,” *J Solid State Chem*, vol. 317, Jan. 2023, doi: 10.1016/j.jssc.2022.123679.

[96] G. Ziyatdinova, E. Guss, and E. Yakupova, “Electrochemical sensors based on the electropolymerized natural phenolic antioxidants and their analytical application,” *Sensors*, vol. 21, no. 24. MDPI, Dec. 01, 2021. doi: 10.3390/s21248385.

[97] B. Qiu, J. Wang, Z. Li, X. Wang, and X. Li, “Influence of acidity and oxidant concentration on the nanostructures and electrochemical performance of polyaniline during fast microwave-assisted chemical polymerization,” *Polymers (Basel)*, vol. 12, no. 2, Feb. 2020, doi: 10.3390/polym12020310.

[98] R. A. Lorenzo, A. M. Carro, C. Alvarez-Lorenzo, and A. Concheiro, “To remove or not to remove? The challenge of extracting the template to make the cavities available in molecularly imprinted polymers (MIPs),” *International Journal of Molecular Sciences*, vol. 12, no. 7. pp. 4327–4347, Jul. 2011. doi: 10.3390/ijms12074327.

[99] M. Elshiaty, H. Schindler, and P. Christopoulos, “Principles and current clinical landscape of multispecific antibodies against cancer,” *International Journal of Molecular Sciences*, vol. 22, no. 11. MDPI, Jun. 01, 2021. doi: 10.3390/ijms22115632.

[100] M. F. Frasco, L. A. A. N. A. Truta, M. G. F. Sales, and F. T. C. Moreira, “Imprinting technology in electrochemical biomimetic sensors,” *Sensors (Switzerland)*, vol. 17, no. 3. MDPI AG, Mar. 06, 2017. doi: 10.3390/s17030523.

[101] R. S. Gomes, F. T. C. Moreira, R. Fernandes, and M. F. Goreti Sales, “Sensing CA 15-3 in point-of-care by electropolymerizing O-phenylenediamine (oPDA) on Au-screen printed electrodes,” *PLoS One*, vol. 13, no. 5, May 2018, doi: 10.1371/journal.pone.0196656.

[102] Y. J. Li *et al.*, “Constructing electrochemical sensor using molecular-imprinted polysaccharide for rapid identification and determination of L-tryptophan in diet,” *Food Chem*, vol. 425, Nov. 2023, doi: 10.1016/j.foodchem.2023.136486.

[103] “Introduction to the Fundamentals of Raman Spectroscopy.”
[104] M. I. Boyer, S. Quillard, G. Louarn, G. Froyer, and S. Lefrant, “Vibrational study of the FeCl3-doped dimer of polyaniline; a good model compound of emeraldine salt,” *Journal of Physical Chemistry B*, vol. 104, no. 38, pp. 8952–8961, Sep. 2000, doi: 10.1021/jp000946v.
[105] G. V. Martins, A. C. Marques, E. Fortunato, and M. G. F. Sales, “8-hydroxy-2’-deoxyguanosine (8-OHdG) biomarker detection down to picoMolar level on a plastic antibody film,” *Biosens Bioelectron*, vol. 86, pp. 225–234, Dec. 2016, doi: 10.1016/j.bios.2016.06.052.
[106] A. Mohammed and A. Abdullah, “SCANNING ELECTRON MICROSCOPY (SEM): A REVIEW.”
[107] X. Zhu, M. M. Olsson, R. Bajpai, K. Järbrink, W. E. Tang, and J. Car, “Health-related quality of life and chronic wound characteristics among patients with chronic wounds treated in primary care: A cross-sectional study in Singapore,” *Int Wound J*, vol. 19, no. 5, pp. 1121–1132, Aug. 2022, doi: 10.1111/iwj.13708.
[108] “W O U N D E X U D A T E.” [Online]. Available: www.woundsinternational.com
[109] K. F. Cutting, “Wound exudate: composition and functions,” *Br J Community Nurs*, vol. 8, no. Sup3, pp. S4–S9, Sep. 2003, doi: 10.12968/bjcn.2003.8.Sup3.11577.